Asymmetric Effects of Anodal Transcranial Direct Current Stimulation on Intrinsic Connectivity in the Left and Right Dorsolateral Prefrontal Cortex

By

Zachary Angus McAllister

A Thesis Submitted to The Faculty of Graduate Studies of

The University of Manitoba

In Partial Fulfillment of the Requirements of the Degree of

MASTER OF SCIENCE

Department of Human Anatomy and Cell Science

University of Manitoba

Winnipeg, Manitoba

Copyright © 2023 Zachary McAllister

Abstract

Transcranial direct current stimulation (tDCS) applied to the dorsolateral prefrontal cortex (DLPFC) has been shown to have asymmetric behavioral effects, but the underlaying neurophysiological mechanisms causing these asymmetric behavioral differences are poorly understood. Functional magnetic resonance imaging (fMRI) can be used in conjunction with a behavioral measurement to better understand these mechanisms. To measure the hemispheric laterality of neurophysiological and behavioral effects of anodal tDCS applied to the left and right DLPFC using fMRI and Stroop test interference, 11 male and 28 female healthy participants were randomized into three treatment groups of 1.5mA anodal tDCS applied to sham or the left or right the DLPFC, with the cathode placed on the contralateral supraorbital region. Before and after tDCS application participants took the Stroop test and underwent resting-state fMRI. Seed-to-voxel functional connectivity and voxel-to-voxel whole brain intrinsic connectivity (IC) analyses were performed on the fMRI data. All fMRI analysis was done by using two sets of 2×2 factorial analyses between groups (real vs. sham) and time (pre- vs. post-tDCS) for each left and right tDCS, separately, while Stroop interference was measured using a repeated measures general linear model. tDCS to the left DLPFC in the voxel-to-voxel analysis resulted in three significant clusters of changed IC, with one of the clusters being an increase of IC in the left prefrontal region. tDCS to the right DLPFC in the voxel-to-voxel analysis resulted in only one significant cluster of decreased IC in the right prefrontal region. For Stroop interference, only tDCS to the right DLPFC improved Stroop interference performance with left and sham causing no significant changes. No significant changes were found for seed-to-voxel analysis. This study shows that tDCS applied to the left and right DLPFC causes asymmetric changes to IC, as well as providing further support that the DLPFC is asymmetric in interference control, with only tDCS to the right DLPFC having a significant effect on interference.

Keywords

tDCS, DLPFC, fMRI, Stroop Test, Hemispheric Asymmetry, Intrinsic Connectivity

Acknowledgements

I would like to express my sincere gratitude to my supervisor, Dr. Ji Hyun Ko, whose unwavering patience and invaluable guidance have been instrumental throughout the writing of my thesis. His consistent availability and timely feedback have been truly appreciated.

I am also immensely grateful to our esteemed lab post-doc, Dr. Tiffany Carther-Krone, for her exceptional dedication in aiding with various forms of analysis, reviewing my writing, and addressing any questions I had. Her commitment has gone above and beyond the call of duty.

I would like to extend my appreciation to the individuals within our lab group who have generously supported me. Dr. Iman Beheshti, for providing invaluable assistance with SPSS analysis; Dr. Tiffany Kolesar, for her valuable guidance with CONN and pCASL analysis; and Natalie Wright, for her assistance with ANAM and helping me navigate other behavioral tests. Additionally, I would like to acknowledge Eun Choi, our lab research assistant, for her invaluable support in addressing any queries I had regarding data collection.

I would like to express special thanks to my advisory committee members, Dr. Katinka Stecina and Dr. Steven Greening, for their willingness to mentor me and for their thorough review and insightful suggestions for my writings.

Lastly, I would like to extend my heartfelt gratitude to all the current and former members of our lab group for their remarkable kindness, unwavering support.

Table of Contents

Abstract i

Acknowledgements ii

Table of Contents iii

List of Tables v

List of Figures vi

List of Abbreviations vii

1. Introduction 1

2. Background 4

2.1 Transcranial Direct Current Stimulation 4

2.1.1 Brief History of Transcranial Direct Current Stimulation 5

2.1.2 Clinical Applications of Transcranial Direct Current Stimulation 6

2.1.3 Brief Explanation of Action Potentials and Neuronal Firing 7

2.1.4 Physiology of Transcranial Direct Current Stimulation 11

2.1.5 Hemispherical Asymmetric Effects of Transcranial Direct Current Stimulation 16

2.2. The Dorsolateral Prefrontal Cortex 17

2.2.1 Role of the Dorsolateral Prefrontal Cortex 18

2.2.2 Transcranial Direct Current Effects on the Dorsolateral Prefrontal Cortex 21

2.3 Functional Neuroimaging Techniques 22

2.3.1 Functional Magnetic Resonance Imaging 24

2.3.2 Pseudo-Continuous Arterial Spin Labeling 27

2.3.3 Transcranial Direct Current Stimulation, the Dorsolateral Prefrontal Cortex and Neuroimaging 29

3. Aim, Objectives, and Hypothesis 34

4. Methods 36

4.1 Study Participants 36

4.2 Stroop Test Administration 36

4.3 Application of tDCS and Neuroimaging 38

4.4 Behavioral Data Analysis 39

4.5 fMRI Functional Connectivity Analysis 40

4.6 pCASL Cerebral Blood Flow Analysis 41

5. Results 43
5.1 Demographic Analysis 43
5.2 tDCS Effects on Interference Score 43
5.3 Functional Connectivity Analysis with A Priori Regions of Interest 44
5.4 Voxel-to-Voxel Intrinsic Functional Connectivity Analysis 45
5.4.1 Functional Connectivity Analysis with Intrinsic Connectivity Clusters 47
5.5 pCASL Cerebral Blood Flow Analysis 48
6. Discussion 49
7. Limitations and Future Directions 53
8. Conclusion 54
References 55

List of Tables

Table 1. Summary of studies applying tDCS to the DLPFC 32
Table 2. Demographic information for participants 43
Table 3. Summary of fMRI IC results 46

List of Figures

Figure 1. Transcranial Direct Current Setup....4
Figure 2 Overview of a MEP....6
Figure 3 Anatomy of a Neuron....9
Figure 4 Overview of an Action Potential....10
Figure 5. Propagation of an Action Potential in Myelinated Neuron....11
Figure 6. Stochastic Resonance....14
Figure 7. Location of the Dorsolateral Prefrontal Cortex....18
Figure 8. Overview of Various Methods of fMRI Functional Connectivity Analysis....27
Figure 9. Overview of the Steps of Arterial Spin Labeling....29
Figure 10. Stroop Test....37
Figure 11. tDCS Target Location....38
Figure 12. ΔInterference Score Post vs. Pre tDCS....44
Figure 13. Changes in IC Following the tDCS:....47

List of Abbreviations

ACC	Anterior Cingulate Cortex	**IR**	Inversion Recovery
AMPA	α-amino-3-hydroxy-5-methyl-4-isoxazolepropionic acid	**LTD**	Long-term Depression
ANAM	Automated Neurophysiological Assessments Metrics	**LTP**	Long-term Potentiation
BDI-II	Beck Depression Inventory II	**M1**	Primary Motor Cortex
BDNF	Brain-derived Neurotrophic Factor	**MEPs**	Motor Evoked Potential
BOLD	Blood-oxygen Level-dependent	**MFG**	Middle Frontal Gyrus
CaMKII	Ca2+/Calmodulin-dependent Protein Kinase-II	**MNI**	Montreal Neurological Institute
cAMP	Cyclic adenosine monophosphate	**MoCA**	Montreal Cognitive Assessment
CBF	Cerebral Blood Flow	**NIBS**	Non-invasive Brain Stimulation
CREB	cAMP Response Element-Binding Protein	**NMDA**	N-methyl-D-aspartate
CSF	Cerebral Spinal Fluid	**pCASL**	Pseudo-continuous Arterial Spin Labeling
DLPFC	Dorsolateral Prefrontal Cortex	**PET**	Positron-emission Tomography
DMN	Default Mode Network	**ROI**	Region of Interest
EEG	Electroencephalographic	**rTMS**	Repetitive Transcranial Magnetic Stimulation
FEM	Finite Element Method	**TI**	Inversion Time
fMRI	Functional Magnetic Resonance Imaging	**tDCS**	Transcranial Direct Current Stimulation
FOV	Field of View	**TE**	Echo Time
GABA	*gamma*-aminobutyric acid	**TR**	Repetition Time
IC	Intrinsic Connectivity	**WCST**	Wisconsin Card Sorting Task
ICA	Independent Component Analysis		

1. Introduction

Transcranial direct current stimulation (tDCS) is one of the most widely used non-invasive brain stimulation techniques (NIBS). It introduces a unique capacity to manipulate neuronal excitability allowing "perturbing and measuring" of brain activity and functions. As a painless, affordable and portable brain stimulation technology, tDCS produces long lasting effects when applied repeatedly and is often used to improve symptoms in individuals with brain disorders such as fibromyalgia, depression and tinnitus.[1]

Early studies elucidating the neurophysiological mechanisms of tDCS began by studying the motor evoked potentials (MEPs) resulting from the stimulation of the motor cortex.[2,3] MEPs are typically measured using electromyography (EMG), which involves placing surface electrodes on muscles that are innervated by spinal motor neurons which receive input from the motor cortex, such as the first dorsal interosseous muscle. The MEPs can be quantified in terms of their amplitude and latency, which can provide information about the excitability of the motor cortex and the integrity of the motor pathway. The motor cortex has been shown to be a symmetric region in terms of the effects of tDCS on MEPs, especially when hemispheric dominance and handedness are considered. For example, applying anodal tDCS to the left or right primary motor cortex (M1) both resulted in significant increases to MEP amplitudes, while cathodal stimulation on each of the hemispheres both resulted in significant decreases in MEP amplitudes.[4] The effects of the tDCS are also consistently localized to the target hemisphere. One study found tDCS to the left M1 changes the amplitude of MEPs originating from the left M1 but has no significant effect on MEPs originating from the right M1.[5] However, beyond the motor cortex the hemispherical symmetry of tDCS effects is not necessarily substantiated. In prefrontal regions like the dorsolateral prefrontal cortex (DLPFC) it has been found that targeting the left DLPFC with tDCS causes an increase in pupil dilation, while targeting the right DLPFC causes a decrease.[6]

Hemispherical asymmetry in behavioral responses to tDCS has also been found for inhibition [7,8], verbal memory [9] and initial thinking time.[10]

This contrast between the symmetric effects of tDCS on M1 MEPs and the often-asymmetric effects when targeting prefrontal regions is an issue in understanding the neurophysiological mechanisms of prefrontal tDCS because the findings on M1 MEPs may not be necessarily transferable to prefrontal regions. Understanding the effects of tDCS (or NIBS in general) on the prefrontal cortex specifically is important due to it being a commonly targeted region to treat drug-refractory neuropsychiatric brain disorders such as schizophrenia [11] and depression.[12]

However, it has not yet been fully understood why left vs. right DLPFC stimulation can have opposite behavioral or neurophysiological responses. These lateralized effects of NIBS have often been attributed to the lateralized functional role of the DLPFC.[13] Another possibility that has not yet extensively been postulated is whether the neurophysiological properties in response to NIBS themselves could be opposite depending on the location of the stimulation. [14]For example, prefrontal NIBS-induced changes in synaptic dopamine release in striatal and extrastriatal regions were asymmetrical between hemispheres.[15,16]

In this study, to compare the different neurophysiological effects of anodal tDCS on left vs. right DLPFC, we performed a tDCS-fMRI study with healthy individuals. Participants were scanned with resting-state fMRI to measure the functional connectivity before and after 15-minutes of tDCS. Participants were also behaviorally assessed with the Stroop test, which is known to be associated with inhibition control [17] and DLPFC function.[18] The Stroop test is considered a “gold standard” of measuring the activity of the DLPFC as neuroimaging functional magnetic resonance imaging (fMRI) have shown increased activation in the DLPFC during the Stroop test, particularly when participants are faced with incongruent trials.[19] Furthermore, studies involving brain stimulation techniques like excitatory high-

frequency repetitive transcranial magnetic stimulation (rTMS) have demonstrated that improving DLPFC function can improve Stroop performance, further highlighting its involvement in the task.[20]

2. Background

2.1 Transcranial Direct Current Stimulation

The apparatus used for transcranial direct current stimulation or tDCS is composed of two electrodes, an anode and cathode, as well as an energy source which is usually a battery. A plastic head band can be used to hold the anode and cathode pads or saline-soaked sponges in place while they are placed on the head. When the anode pad or sponge is applied to the target area, it is said to be under “anodal” stimulation while the reverse is true for the cathode pad. As a general principle, anodal stimulation increases the physiological response from the target area, while cathodal stimulation is inhibitory (see Figure 1 for an example of a tDCS setup).



Figure 1. Transcranial Direct Current Setup: Two-saline soaked sponges were attached to electrodes (anode red, cathode blue) which were then attached to a battery-powered device capable of modulating current intensity and duration.

2.1.1 Brief History of Transcranial Direct Current Stimulation

In its most rudimentary form, transcranial stimulation has been in use for centuries going back to at least the Roman era with the torpedo fish. *Torpedo* is a genus of stingray found in the warm waters of the Mediterranean capable of producing electric shocks, and is recorded to have been used by the Roman's to treat headaches[21]. The first known use of tDCS by using a galvanic battery and electrode occurred in 1801 when Giovanni Aldini used the technique to treat the major depression of a local farmer. The further use and study of tDCS continued throughout the 19th- early 20th century, however the inconsistency in procedure and few details on the parameters of the application of tDCS made studies of this era difficult to follow and reproduce.[22]

The modern era of the investigation of tDCS began in earnest by studying the motor evoked potentials (MEPs) resulting from the stimulation of the motor cortex.[2,3] The MEPs can be quantified in terms of their amplitude and latency, which can provide information about the excitability of the motor cortex and the integrity of the motor pathway (see Figure 2 for an overview of a MEP). By measuring MEPs before, during, and/or after tDCS, researchers can gain insights into how tDCS modulates the excitability of the motor cortex and associated motor pathways, and how these changes may relate to the desired effects of tDCS. The early tDCS MEP studies found that the placement of the anode to motor cortex increased the resulting MEPs in muscle of the right hand of the participants, while cathodal stimulation decreased it. Due to the advantages of tDCS like it being affordable, non-invasive with mild aversive effects and easy to use, and the reproducibility shown by studies on the motor cortex, tDCS has come under increasing research interest in recent times.

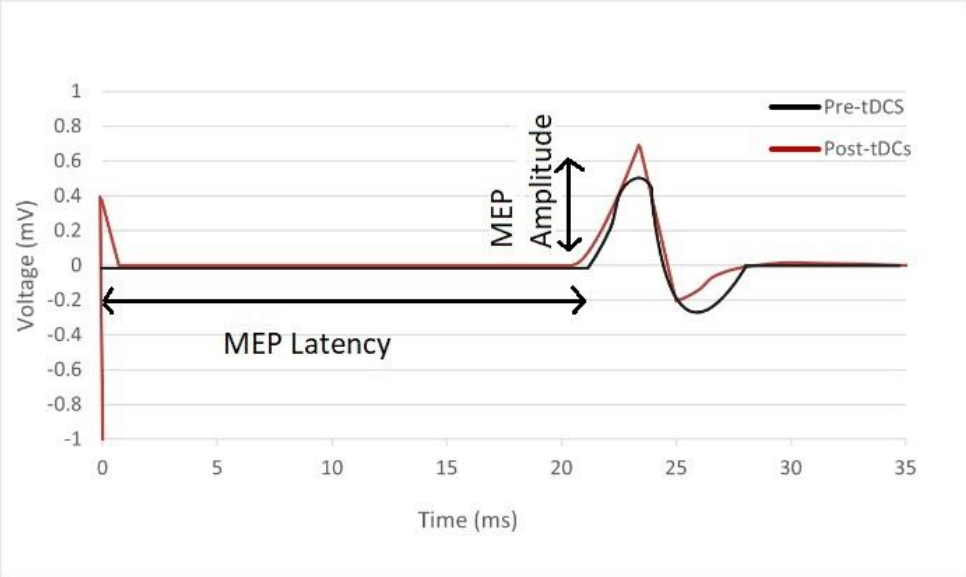


Figure 2 Overview of a MEP: The latency of a MEP is the time it takes for the MEP to occur after the stimulation is applied. It is typically measured in milliseconds (ms) and reflects the time it takes for the electrical signal to travel from the site of stimulation in the brain to the target muscle. The amplitude of a MEP refers to the strength or magnitude of the MEP response, and it is typically measured in millivolts (mV). It reflects the magnitude of the electrical activity in the muscles in response to the stimulation. In this example figure, tDCS increased the MEP latency and amplitude (Adopted and modified from Hirano et al, 2016).[23]

2.1.2 Clinical Applications of Transcranial Direct Current Stimulation

Currently, tDCS has been approved by Health Canada as a treatment for pain mitigation in fibromyalgia and migraine, allowing patients to receive treatment administered by health-care professionals. For treating migraine, the cathode is usually placed on the occipital cortex, which is known to be hyper-active in migraine patients.[24] For fibromyalgia the primary motor cortex M1 is targeted due to the findings of both transcranial magnetic stimulation (TMS) and some tDCS studies that have showed a reduction in fibromyalgia pain when targeting this area.[25]

However, most clinical applications of tDCS are “off-label’, having not yet received official approval of specific indication from Health Canada. One of the most promising clinical applications of tDCS is its effects in treating depression. Many studies have found that tDCS can lead to significant

improvements in treating depression in clinical[26] and at home settings[27] although there is some variability in the effect size between the studies. In most instances the anode is placed over the left dorsolateral prefrontal cortex (DLPFC) while the cathode is placed over the right DLPFC. This is due to the findings of various studies that right DLPFC hyperactivity is correlated with depression severity, while left DLPFC hypoactivity has been correlated with negative emotional judgement.[13]

Exploration has also been done in the applications of tDCS in reducing craving in drug addiction[28,29], and improving symptoms for Alzheimer's disease[30] and schizophrenia.[11] For drug addiction, a primary targeted region for tDCS is the DLPFC due to its known role in inhibitory control.[31] Despite finding an improvement in symptoms in reducing drug craving[28,29], much work still needs to be done to understand the underlaying neurophysiological mechanisms causing these improvements.

The investigation of tDCS for improving recognition memory and general cognitive function in Alzheimer patients generally targets the temporoparietal cortex and the DLPFC.[32] However, regardless of numerous studies finding improvements in working memory and other cognitive deficits due to Alzheimer's, there is still a high level of inconsistency in these results.[33] Similarly for schizophrenia, studies have shown improvement in negative and positive symptoms, such as emotional blunting and hallucinations respectively, however these results are not consistent across all studies[34].

Overall, tDCS has a wide range of possible clinical uses and is primarily targeted to prefrontal and temporal regions. Nonetheless, a lack of consistency between study results and a gap in understanding the underlaying neurophysiological mechanisms that are responsible for these findings are areas in need of improvement to increase the clinical applicability of tDCS.

2.1.3 Brief Explanation of Action Potentials and Neuronal Firing

When a neuron is at a state of rest, Na+ and Cl- are in higher concentrations outside of the cell, but K+ is at higher concentration inside the cell. The Na+/K+ pump expends energy to move Na+ out of the cell

against its electrical and chemical concentration gradients, and K+ into the cell against its chemical concentration gradient. Due to the neuronal membrane being more permeable to K+ and Cl- than Na+ when at a state of rest, this leads to some of the K+ to follow its chemical gradient out of the membrane and Cl- to follow its chemical gradient into the cell. Of course, this movement of K+ and Cl- ions to follow their chemical gradients is counteracted by the electrical gradient it produces, but the ultimate homeostasis created by the electrochemical gradients of these ions is a negative resting membrane potential of around -70mv.[35] However, when excitatory neurotransmitters from other neurons cross a synapse and bind to receptors on the dendrites of the target neuron, this causes the opening of Na+ ion channels and allows Na+ into the cell depolarizing it (see Figure 3 for an anatomical overview of a neuron). If this depolarization is sufficient to reach the activation threshold potential of around -55mv, all Na+ channels at the axon hillock will open, completely depolarizing the neuron membrane to around +40mv.[36]

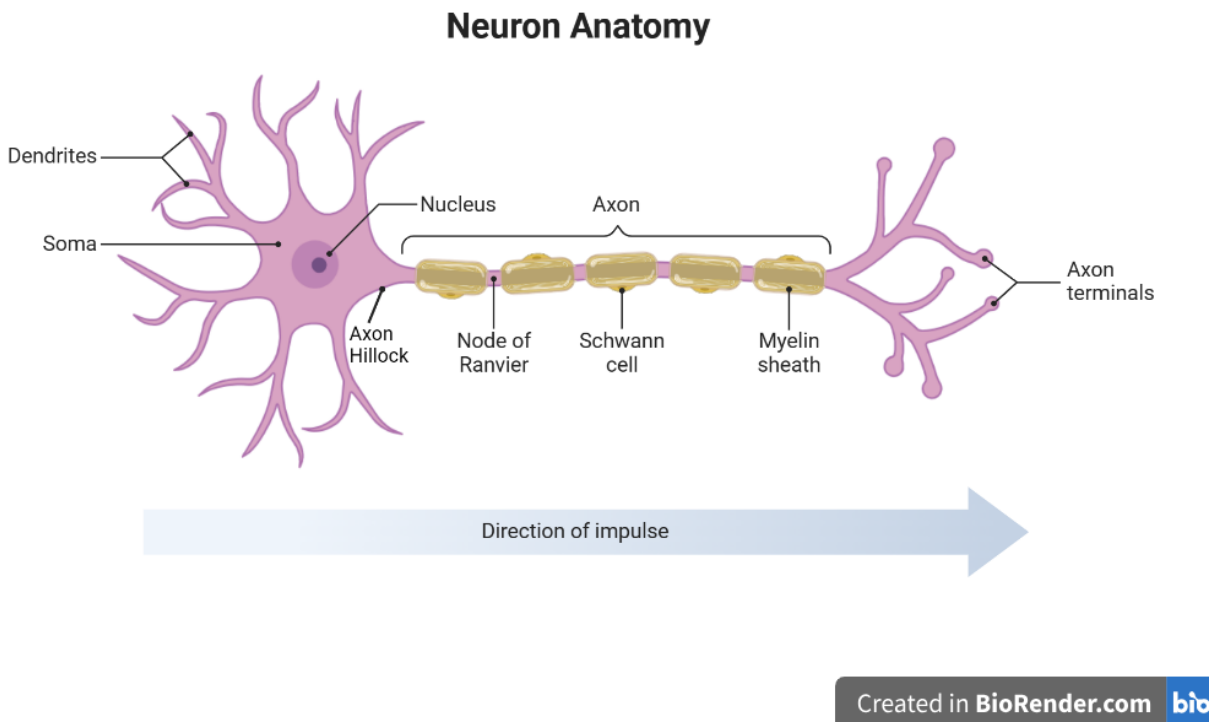


Figure 3 Anatomy of a Neuron: Action potentials begin in the axon hillock after a sufficient level of depolarization opens the Na+ ion channels. Created in BioRender.

The complete depolarization and the opening of the Na+ channels of the axon hillock is an "all or nothing" event, in which subthreshold depolarization will not cause the propagation of an action potential (see Figure 4 for an overview of an action potential). At the peak of complete depolarization, the Na+ channels close via an inactivation gate that plugs the channel pore. These gates are insensitive to changes in polarization and thus the neuronal membrane enters the absolute refractory period, where any further depolarization will not cause neuronal firing. Simultaneously, K+ ion channels open allowing K+ ions to exit the cellular membrane and begin to repolarize it. Due to the slow speed that the K+ ion channels close in response to the repolarization, it leads to a state of hyperpolarization, where the cell-membrane is more negative than its resting potential. It is during this time that the inactivation

gates of the Na+ channels reopen, allowing the propagation of new action potentials, however, because the neuronal membrane is hyperpolarized it takes more depolarization for it to reach the threshold activation potential. This state is known as the relative refractory period. Eventually K+ leakage channels and the Na+/K+ ATPase pump returns the neuronal membrane back to its resting membrane potential.

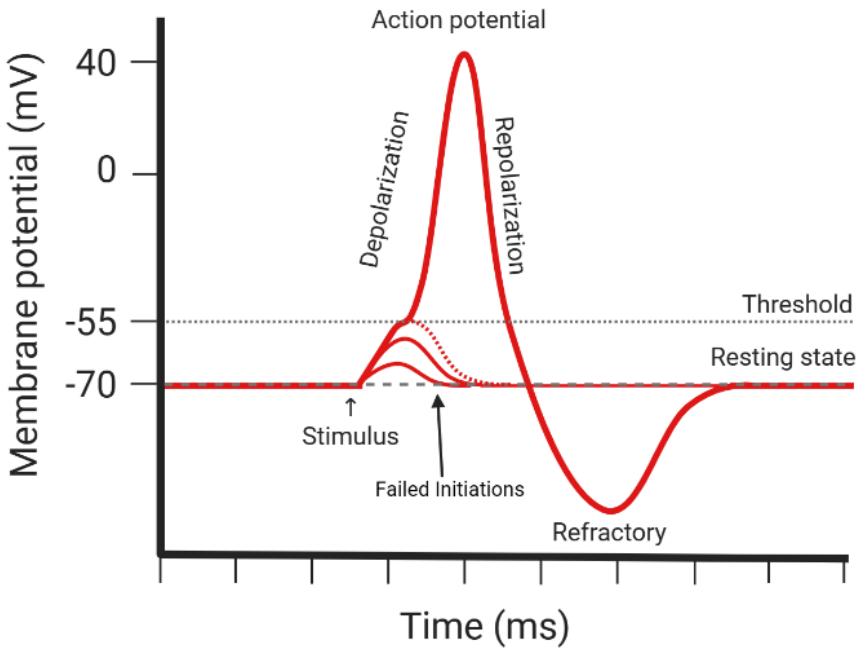


Figure 4 Overview of an Action Potential: Approximate timeline for the stages of an action potential. (Adopted from Khanna, 2021).[37] Created in BioRender.

When the depolarization reaches the threshold required for Na+ channels to open in the axon hillock, it causes a "domino" effect, opening Na+ ion channels down-stream and furthering the depolarization down the axon (see Figure 5 for an illustration). Eventually, the depolarization reaches the axon terminals, where it causes the release of neurotransmitters that then transmit the signal to the post-synaptic neuron, potentially causing the propagation of another action potential.

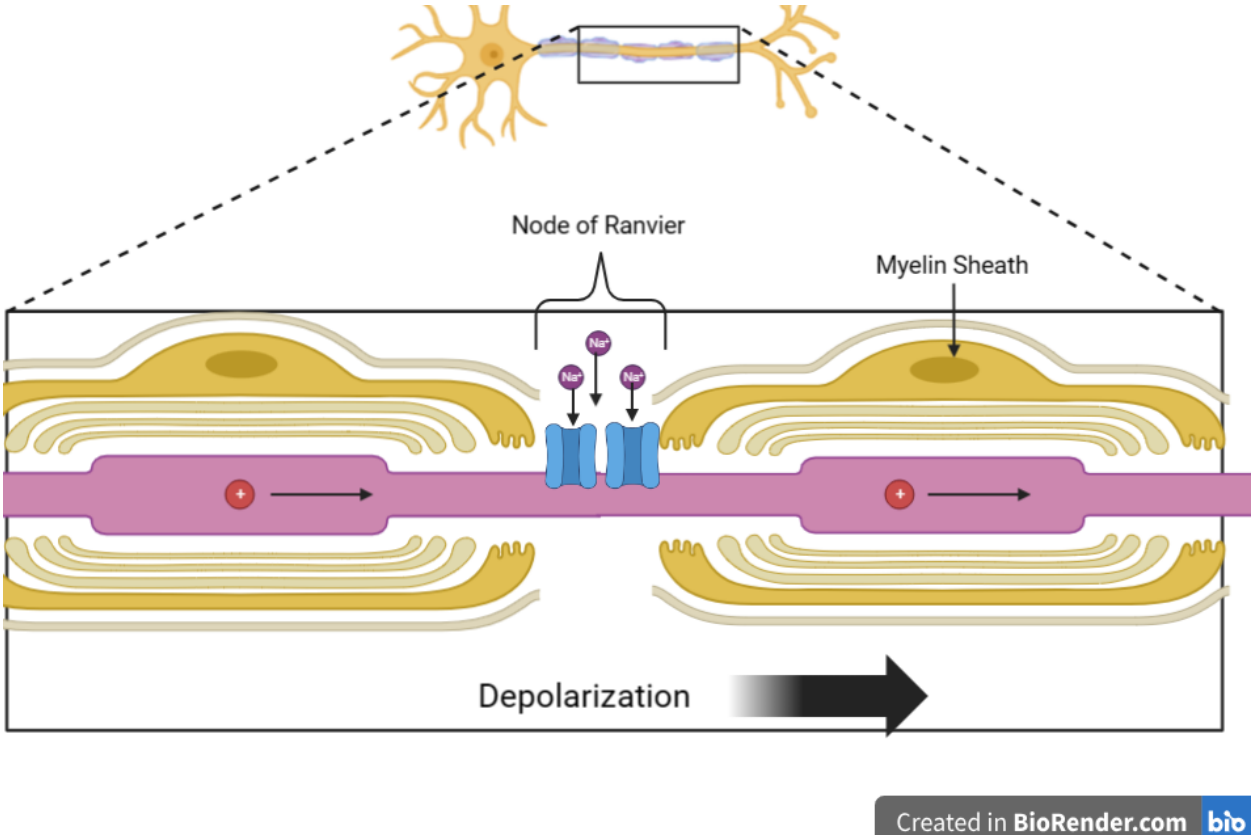


Figure 5. Propagation of an Action Potential in Myelinated Neuron: Threshold depolarization of the neuronal membrane in one node of Ranvier allows it to conduct this depolarization quickly to another node, helping it meet its threshold potential to open voltage-gated sodium ion channels and further propagate the action potential down the neuron. (Adopted from Bill Yates, 2023).[38] Created in BioRender.

2.1.4 Physiology of Transcranial Direct Current Stimulation

In tDCS, the current applied by the anode to the cathode travels through the scalp to reach the cortex, diminishing the current by approximately 90%.[39] Nevertheless, the current that is conducted by the cortical tissue produces an electric field, which is believed to cause depolarization or hyperpolarization to the neuronal membranes depending on their orientation to that electric field.[40] Depolarization of the neuronal membrane by tDCS does not directly cause the neuron to fire an action potential as the changes in potential are not sufficient to reach the activation threshold potential, it only increases the likelihood of it to do so, while hyperpolarization has the opposite effect.

As a general principle, anodal stimulation increases the physiological response from the target area, while cathodal stimulation is inhibitory. However, this is not always the case as there have been instances when cathodal stimulation increases neuronal activity in the target region.[41] Targeting of the neurophysiological effects of the stimulation is another issue. Studies have found that the peak electric current 'hotspots' are not necessarily directly under the target electrode[42] and that neurophysiological responses to stimulation can occur in distant regions possibly due to cascading effects of neuronal pathways.[43] Also, due to the gyri and sulci of the brain, different neurons will have different orientations to the electric field in the target area. This means different parts of the target area will be simultaneously either depolarized or hyperpolarized by the electric field.[14] Interindividual differences in the anatomy of participants also makes targeting difficult and can dramatically change the resulting neurophysiological effects.[44]

It is of interests that tDCS tends to have consistent macro physiological and/or behavioral responses, such as increased blood flow in the target area[45] or increased working memory[46] despite of the inter-individual variabilities in anatomy which may results in inconsistent targeting. One theory postulated by de Berker et al.[14] is that it causes macro-level effects through stochastic resonance. The basis of this theory is that tDCS introduces neural noise that strengthens a neurophysiological response. Because the neural noise is random, and the macro neurophysiological response is non-linear and requires a threshold to activate, the addition of neural noise may help a group of neurons to reach that macro-threshold for activation of that larger physiological or behavioral response.[47] In this scenario, with a small amount of additional noise, it is only the neuron clusters closest to causing a macro neurophysiological response prior to the application of tDCS that can reach the threshold, while most neuronal groups farther from threshold produce no macro neurophysiological response from the tDCS (see Figure 6 for a depiction of stochastic resonance). In theory, too much noise would then cause more neuronal groups to fire and muddle and weaken the macro neurophysiological response, however there

is a gap in the literature on the effects of increased current intensities and resulting electric fields on human subjects. One study found no significant differences in cortical excitability between tDCS currents of 1mA and 2mA[48], but it is not clear if 2mA is an intensity sufficient to create enough neural noise to depress a macro neurophysiological response. In fact, 1-2mA is the current intensity used in the majority of tDCS study to try to elucidate macro neurophysiological changes induced by tDCS. Higher current intensities are therefore probably required, but most studies that use higher current intensities are testing the safety of those currents[49], not the effect they have on the neurophysiological response. Stochastic resonance is an interesting theory as to why the introduction of a neural noise through tDCS can cause macro neurophysiological changes, but it still needs further development.

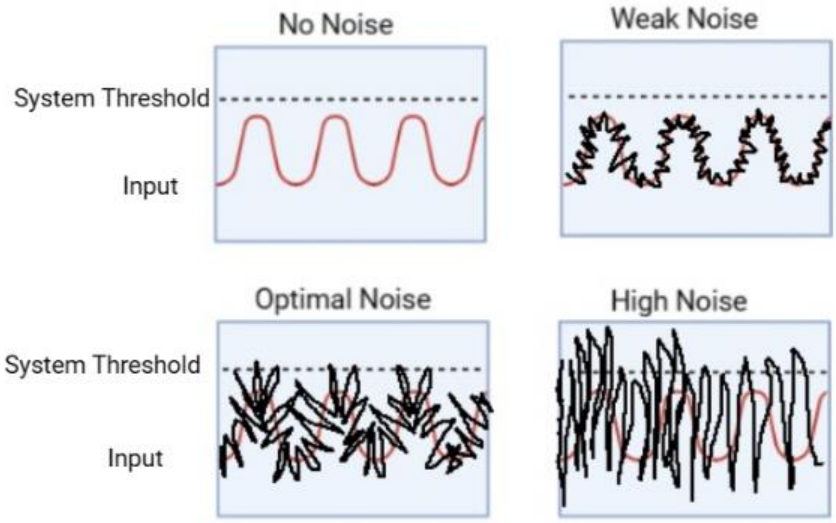


Figure 6. Stochastic Resonance: The addition of optimal amount of noise can cause a subthreshold input to reach the system threshold periodically, while still maintaining the same sinusoidal wave. However, too much noise can make the input signal indistinguishable. (Adopted from Groen et al, 2018).[50]Created in BioRender

The electric fields induced by tDCS that increase neuronal firing are believed to be responsible for the most acute macro neurophysiological effects. However, tDCS has been shown to be capable of causing significant behavioral effects lasting hours[51] to week[52] after application, which is thought to be due to long-term changes to synaptic plasticity.[53] Changes in synaptic plasticity can be divided into early phase, which is reported to be responsible for observed changes up to six hours, and a late phase which is capable of making changes to neuronal pathways and excitability that can last days.[54]

The underlaying mechanisms of early phase changes to neural plasticity due to the application of tDCS are not yet fully understood, but there is evidence of increased calcium levels after tDCS[55] and an increase in BDNF that increases the activity of NMDA receptors that is responsible for those increased calcium levels.[56] In the case of early phase long-term potentiation (LTP), increased calcium causes increased activity of the CaMKII enzyme, which then phosphorylates AMPA receptors increasing their activity.[57] Increased activity of the AMPA receptors then increases the rate of sodium entering the neuronal membrane, increasing the extent of depolarization and making the neuron more likely to fire in the future.[58] In the case of early phase long-term depression (LTD), elevated calcium levels bind to calcineurin which then ultimately leads to the dephosphorylation and decreased activity of AMPA receptors[59], decreasing the extent of depolarization and making it more difficult for the neuron to reach the threshold potential.

Late phase LTP and depression involve changes to protein synthesis to make longer lasting changes to synaptic plasticity. In the case of late phase LTP, prolonged high frequency stimulation activates the cAMP dependent protein kinase A and cAMP-response element binding protein (CREB) that ultimately leads to protein synthesis and the insertion of more AMPA and NMDA receptors into the neural synapse.[60] In comparison, late phase LTD involves a calcium signaling cascade that results in the recruitment of adaptor protein 2 and protein kinase C that assists with dephosphorylating the AMPA receptors. This process also requires protein synthesis and eventually results in the endocytosis of AMPA receptors from the synaptic membrane for recycling or degradation.[61]

It should be noted that tDCS intensity, duration, polarity and number of sessions can all effect whether LTP or LTD occurs.[60]There is also some evidence that tDCS can affect neurogenesis in mouse and rat models[62-64], opening the possibility that tDCS can also cause long-term changes to neuronal activity by modulating neuronal architecture.

2.1.5 Hemispherical Asymmetric Effects of Transcranial Direct Current Stimulation

tDCS has been shown to have varying degrees of asymmetry depending on what region is specifically targeted. As previously stated in the history of tDCS, the modern study of the neurophysiological effects of tDCS began by the study of MEPs when targeting the motor cortex. The motor cortex has been shown to be a symmetric region in terms of the effects of tDCS on MEPs. For example, applying anodal tDCS to the left or right primary motor cortex (M1) both resulted in significant increases to MEP amplitudes, while cathodal stimulation on each of the hemispheres both resulted in significant decreases in MEP amplitudes.[4] The effects of the tDCS are also consistently localized to the target hemisphere. Furthermore, studies have found that tDCS to the left M1 changes the amplitude of MEPs originating from the left M1 but has no significant effect on MEPs originating from the right M1.[5]

This hemispherical symmetry of tDCS effects is not necessarily the case though for prefrontal regions like the DLPFC. For example, targeting the left DLPFC with tDCS has been shown to cause an increase in the pupil dilation, while targeting the right DLPFC has shown to cause a decrease.[6] Hemispherical asymmetry in behavioral responses to tDCS has also been found for inhibition[7,65], verbal memory[9] and initial thinking time.[10] Functional asymmetry in the prefrontal region has also been shown via the electroencephalographic (EEG) frequency changes induced by tDCS. It has been shown that anodal tDCS to the left prefrontal region with a contralateral bipolar cathode placement can cause an increase in the mean frequency of brain rhythms, while anodal tDCS to the right prefrontal region causes a decrease in this mean frequency.[66]

However, this difference in symmetry in neurophysiological response to tDCS between the motor cortex and the prefrontal regions may be due more so due to using MEP as the neurophysiological measurement for the motor cortex. For instance, functional magnetic resonance imaging (fMRI) studies on tDCS to the motor cortex have shown that tDCS to the right M1 causes an

elevated level of seed-to-voxel functional connectivity between M1 and the premotor cortex caudate nucleus, which is not replicated in tDCS to the left M1.[67] Furthermore, a study found that anodal and cathodal tDCS to M1 had no significant difference pre and post stimulation on the blood-oxygen-level-dependent (BOLD) signal on M1 and the supplementary motor area regions of interest (ROIs) despite previous findings that anodal and cathodal stimulation to M1 increased and decreased MEPs respectively.[68] This suggests that physiological responses of MEP studies are not always analogous and directly comparable to those of fMRI for the motor cortex. Overall, significant caution must be taken in assuming that tDCS will have symmetric neurophysiological effects in functional measurements other than MEPs.

2.2. The Dorsolateral Prefrontal Cortex

The DLPFC is defined more by its function than by its structure. This has made it less specific in how it is structurally defined, but its location is generally defined to the middle frontal gyrus overlapping Broadman's area 9 and 46 (see Figure 7 for the approximate location of the DLPFC and other nearby brain regions). Due to a considerable number of clinical applications of tDCS targeting prefrontal brain regions, the DLPFC has become an area under increasing interest in which to try to understand the underlaying neurophysiological mechanisms of how tDCS effects the prefrontal regions of the brain.

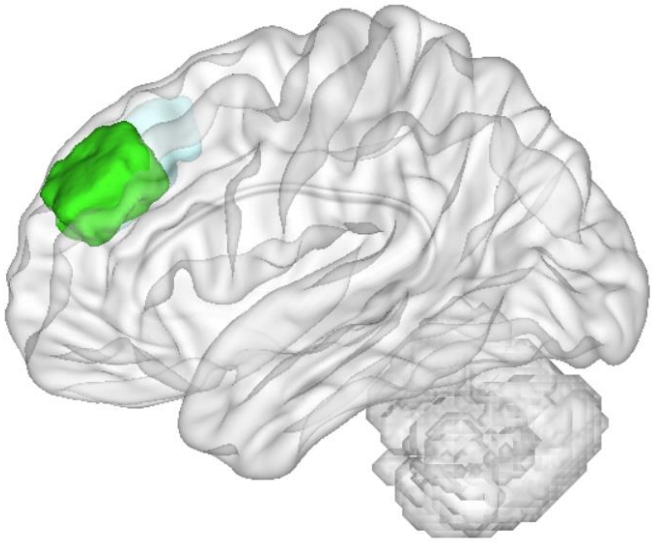


Figure 7. Location of the Dorsolateral Prefrontal Cortex : The DLPFC in green is located on the lateral side of the middle frontal gyrus overlapping Broadman areas 9/46. Constructed using BRANT.[69]

2.2.1 Role of the Dorsolateral Prefrontal Cortex

The DLPFC is a prefrontal brain area that is primarily involved in many executive functions such as working memory, task switching, moral decision making, and inhibition control. Lesion studies on the DLPFC have found significant deficits for working memory[70-72], and increased BOLD signal in the DLPFC during a working memory tasks has also been recorded.[73] The DLPFC's specific role in working memory is still being further elucidated, however, it is believed to be important for the manipulation and monitoring of working memory content more so than the maintenance of working memory itself.[70] Studies on lesions to the human DLPFC have shown that working memory maintenance was not significantly impacted[74,75], yet when increasing the number of items that had to be remembered[75] it lead to a decrease in performance. This dissociation leads credence to the possibility that the DLPFC is monitoring working memory and not maintaining it.

The Wisconsin Card Sorting Test (WCST) is a test on the ability of an individual for rule maintenance and task switching. During the task, the participant must match a card they possess to one of the four or more cards presented that may share an attribute with the card they possess, such as shape, shape colour or number of shapes. The rule of the correct matching attribute is not explicitly stated and must be found by the participant via trial and error, and after several trials the correct matching rule changes. Individuals with damage to the DLPFC have a decreased performance in the WCST as they struggle to change to a new rule when the previously correct rule is no longer valid.[76] Positron Emission Studies (PET) have also found that increased metabolism in the DLPFC is correlated with a decrease in preservation of previous rule errors.[77] These findings suggest that the DLPFC has a functional role in task-switching between behavioral correct rules.

fMRI studies have also shown that the DLPFC has increased activation when individuals are making moral judgements, especially those that require cognitive control and conflict resolution.[78] A tDCS study has also shown that inhibiting the left DLPFC and activating the right DLPFC leads to a decreased capacity of moral reasoning.[79] This suggests that the DLPFC may be involved in regulating emotional responses to moral dilemmas and ensuring that moral decisions are consistent with an individual's moral beliefs and values. However, what is not clear is if this increased activity in the DLPFC is specific to moral decision making or is generalizable to decision making requiring cognitive control. Another fMRI study suggests it may be the later by finding that the bilateral DLPFC was more activated for questions that required a semantic judgement rather than a moral one.[80] Further study still needs to be done to fully elucidate the role of the DLPFC in moral decision making.

The DLPFC is also believed to be a key brain region for inhibition control. Inhibition control is the ability of an individual to override an automatic or prepotent response for a different response that is better orientated to their goals or desires. Inhibitory cathodal tDCS to the left DLPFC has led to worse inhibition performance[81,82], individuals with damage to the DLPFC have reduced inhibition abilities[83] and

anodal excitatory tDCS to the left DLPFC has led to increased inhibition performance.[31] According to the conflict control loop theory, the DLPFC's role in inhibition is to maintain selective attention by supressing irrelevant information while the anterior cingulate cortex (ACC) is believed to participate in error detection.[84] This was finding was due to the DLPFC having an increased fMRI BOLD signal during both the congruent and incongruent colour naming part of the Stroop task (which both requires cognitive control and attention), while the ACC only had significantly more activity during the incongruent colour naming portion of the task (in which the participant must say the correct type colour of the word when the semantic meaning is incongruent, thus requiring conflict monitoring).[84]

The DLPFC is believed to be part of other brain networks as well including the frontoparietal network and to a lesser extent the salience network. Brain networks are interconnected neuron systems in the brain that work together to perform various cognitive functions. These networks can be defined structurally or functionally. Structural definitions of brain networks refer to the structural direct connections between various brain regions. Functional definitions, which include the previously mentioned frontoparietal network and salience network, are defined by statistical dependencies and correlations of functional activity between brain regions that are measured with functional neuroimaging techniques such as fMRI. To better understand functional connectivity and neural imaging techniques see **background section 2.3**. The frontoparietal network is primarily involved with attention, task-switching and working memory and primarily engages the DLPFC, ACC, anterior insula and inferior parietal lobule.[85] The salience network, which is involved in detecting salient stimuli and recruiting other networks often interacts with the DLPFC. Although the DLPFC is not usually considered to be directly part of the salience network, fMRI studies have shown coactivation of the salience network with the DLPFC during tasks that require both cognitive control and emotional processing.[86] This suggests that the DLPFC and the salience network work together to integrate cognitive and emotional information and regulate behavior accordingly.

Overall, the DLPFC is a brain region that is involved in executive functions like working memory, task-switching, inhibition control and decision making. It does not participate in these functions in isolation, but instead through significant connections to various networks and other brain regions primarily in the prefrontal cortex, parietal cortex, basal ganglia and thalamus.[87]

2.2.2 Transcranial Direct Current Effects on the Dorsolateral Prefrontal Cortex

As previously stated, tDCS targeting the DLPFC has caused improvements in the ability of inhibiting prepotent, yet incorrect responses [31,81,82], but it also has been shown to cause a wide range of other behavioral changes. For working memory performance, anodal tDCS to the left DLPFC has led to improvements[88-90] as well as cathodal to the left DLPFC[91] and anodal tDCS to the right DLPFC.[92] However, the inconsistency in findings between studies at times can create confusion. For example, cathodal tDCS to the left DLPFC has been shown to cause a deterioration in working memory performance[88] as well as an improvement.[91] Causes for this discrepancy could be originated from differences in tasks at hand (remembering numbers[88] vs. letters[91]), stimulation intensity (2mA vs 1mA), and/or cathode placement (contralateral supra-orbital vs ipsilateral mastoid). Because tDCS is sensitive to changes in electrode montage, stimulation intensity and duration[93], it can be difficult to directly compare the effects of tDCS, especially on a region that is as hemispherically differentiated as the DLPFC. Therefore, caution and an awareness of differences in methodology must be exercised when comparing results between studies for this brain region and for tDCS more generally.

Other behavioral findings for anodal tDCS to the left DLPFC include improvements in planning[94], word fluency[95] and mental flexibility[96], while anodal tDCS to the right DLPFC has been correlated with improvements in emotion regulation[97], mental flexibility[96] and language comprehension.[98] The wide variety of executive tasks that tDCS can modulate when targeting the DLPFC gives further credence to the fact that the DLPFC is a central hub for many different aspects of cognition and behavior.

A potential explanation as to how tDCS to the DLPFC can cause such a wide variety of behavioral outcomes is that fMRI studies have shown that anodal tDCS to the left DLPFC led to increased functional connectivity within the frontoparietal network and default mode network (DMN).[99] Both the DMN and frontoparietal network perform a wide variety of functions, so any induced changes in their activity could cause a large variety of changes in behavioral outcomes. Other fMRI studies investigating tDCS to the DLPFC have found functional connectivity changes distant from the target site, further highlighting the DLPFC as a highly interconnected region to other brain regions and networks.[100]

tDCS targeting the DLPFC has also caused measured functional changes in other techniques such as pseudo-continuous arterial spin labeling (pCASL) and PET. pCASL studies have shown that targeting the right DLPFC with anodal tDCS causes a significant increase in cerebral blood flow in the lateral prefrontal cortex and midcingulate cortex.[101] A PET study has shown that anodal tDCS to the left DLPFC with cathodal on the right DLPFC led to increased dopamine release in the right striatum and a decrease in dopamine for the left striatum.[102] Similarly, inhibitory TMS to the left DLPFC has been shown to cause a decrease in dopamine in the left striatum, while inhibitory TMS to the right DLPFC had no significant effect.[15] In conjunction, these studies show that while tDCS to the DLPFC can cause functional changes at or near the target region, the physiological response to that tDCS may be different or even the opposite depending on which hemisphere of the DLPFC is targeted. This gives further evidence of the DLPFC as being a hemispherically functionally asymmetrical region.

2.3 Functional Neuroimaging Techniques

Functional neuroimaging techniques used in this study include fMRI and pCASL. Functional connectivity is defined as the temporal coincidence of spatially distant neurophysiological events.[103]In order for two brain regions to exhibit a positive functional connection, the activity of one region will synchronize with that of the other. . Anticorrelated functional connections are the opposite, in which the activity of one

region is anti-synchronous with the other. A decrease in functional connectivity between regions means that there is a breakdown in synchronicity or anti-synchronicity between them, with the temporal activity between the regions becoming more random. Intrinsic connectivity is simply the measurement of functional connectivity during a state of rest or task absence.

Parameters in fMRI and pCASL functional neuroimaging include inversion time (TI), repetition time (TR), echo time (TE), flip angle and field of view (FOV).

TI is the time interval between the inversion pulse and the start of the imaging data acquisition. It is used in inversion recovery (IR) sequences, which are used to suppress certain tissues, such as fat or cerebrospinal fluid, to create contrast in MRI images. TI determines the point at which the longitudinal magnetization of certain tissues is inverted and subsequently recovered during the imaging process, allowing for contrast manipulation in MRI images.

TR is the time interval between successive excitations of the magnetization in MRI. It determines the time taken for the MRI sequence to repeat and acquire a new set of data. Longer TR values result in higher signal-to-noise ratio (SNR) and better T1-weighted contrast, while shorter TR values result in faster image acquisition. TR is an important parameter that affects the contrast, SNR, and acquisition time of MRI images.

TE is the time interval between the excitation pulse and the peak of the MRI signal echo. It determines the time at which the MRI signal is sampled after excitation, and it affects the contrast and image quality of MRI images. Longer TE values result in better T2-weighted contrast, as longer T2 relaxation times are sampled, while shorter TE values result in faster image acquisition.

The flip angle is the angle by which the magnetization is tipped away from its equilibrium position by the radiofrequency (RF) pulse during the excitation phase of an MRI sequence. It is typically expressed in degrees and determines the amount of magnetization that is rotated into the transverse

plane to generate the MRI signal. Larger flip angles result in higher signal intensity and better T1-weighted contrast, while smaller flip angles result in lower signal intensity and better T2-weighted contrast.

The FOV is the physical extent of the imaging volume that is sampled in MRI. It is typically expressed in millimeters and determines the size of the image in the spatial domain. A larger FOV covers a larger anatomical region, but may result in lower spatial resolution, while a smaller FOV covers a smaller anatomical region, but may result in higher spatial resolution.[104]

2.3.1 Functional Magnetic Resonance Imaging

fMRI is a safe, non-invasive, and commonly used method to measure brain function during a task or state of wakeful rest. It has a high spatial resolution, in some cases less than 1mm, but its temporal resolution can be 1-3s for the beginning of the signal and 4-8s until the signal peaks.[105] This delay in the temporal resolution is due to fMRI indirectly measuring neuronal activity via the blood-oxygen-level-dependent (BOLD) signal. According to the neurovascular coupling hypothesis, neuronal activity is closely correlated to cerebral blood flow as oxygenated blood travels to neurons that have fired action potentials in order to replenish glucose and other metabolites to restore resting-state homeostasis and prepare the neuron for future action potentials.[106] Glutamate released from the neuronal firing triggers the smooth muscle of artilleries to vasodilate, causing an oversaturation of oxygenated arterial blood to replenish the neurons and displace venous deoxygenated hemoglobin.[107]

An MRI scanner works by applying a magnetic field that lines up hydrogen protons in water molecules in cerebral spinal fluid, cerebral blood, and tissue. Because protons are positively charged, their spin will align parallel or antiparallel to an externally applied magnetic field if the magnetic field strength is sufficient.[108] A radiofrequency pulse is then omitted that temporarily puts the hydrogen atoms into a higher energy state and magnetization vector that is aligned with the radiofrequency pulse.

As the radiofrequency pulse is turned off, it creates a magnetic field perpendicular to the original field. This perpendicular field then decays over time, and the time it takes for it to decay by a factor of *e* (2.718) is known as the time T2. T2 is the time that is measured during fMRI by the MRI scanner, and paramagnetic deoxygenated hemoglobin disrupts the perpendicular magnetic field and thus decreases T2 time.[109] This creates a measurable difference in T2 time between oxygenated and deoxygenated blood, allowing for the indirect measurement of neuronal activity.

Initially, BOLD fMRI neuroimaging was solely a univariate analysis of regional changes in response to a specific task. This changed in 1995 when Biswal et al discovered low-frequency BOLD fluctuations with a high degree of temporal correlation.[110] Now known as intrinsic functional connectivity, it refers to how different regions of the brain work together and communicate with each other to maintain and update its internal model of the world, which includes simplifying complex information through abstraction and aligning similar patterns.

Intrinsic fMRI functional connectivity analysis has a few advantages in comparison to traditional task-based fMRI neuroimaging. Firstly, it provides insights into the intrinsic, baseline state of brain activity which may not be accurately represented when doing a task. Secondly, it allows for a more hypothesis-free whole-brain connectivity analysis that is not focused on specific task-based regions or networks. Third, differences in intrinsic fMRI BOLD signal between healthy and clinical populations allows for it to be an identifying biomarker for neurological and psychiatric disorders.[111,112] Finally, it reduces subject variability that can arise from differences in task performance.

fMRI functional connectivity analyses can take a myriad of different approaches ranging from seed-to-seed, seed-to-voxel, voxel-to-voxel, and independent component analysis. For these forms of analysis, a “voxel” is a pixel that encapsulates the fMRI signal of the brain, like a pixel in a television but it is 3D rather than 2D. Depending on the resolution of the fMRI and the total brain volume, a single

brain can be composed of 250,000-1,300,000 voxels. A “seed” is a region of interest by anatomical or functional criteria, such as anatomical landmarks, resting-state networks, or activations from tasked based fMRI. Seed-to-seed, seed-to-voxel and voxel-to-voxel analysis use a similar methodology in which the synchronicity of the BOLD fMRI signal is compared between distinct seed regions or voxels. Seed based analysis either looks for functional changes between distinct seed regions in seed-to-seed, or a seed in comparison to the voxels in the whole brain seed-to-voxel analysis. Voxel forms of analysis are generally whole-brain analysis in which a seed region or single voxel cluster are compared to the rest of the voxels in the brain and requires less priori assumptions than a seed-based analysis.

Independent component analysis (ICA) is often used to identify spatially independent patterns of brain activity that reflect coherent and meaningful brain networks. The basic idea of ICA is to decompose the multivariate neuroimaging data into a set of statistically independent components that represent underlying sources of activity or signals in the brain. These components are spatial maps that represent patterns of brain activity across the brain, and associated time courses that represent the temporal dynamics of activity for each component. Like voxel-to-voxel analysis, ICA does not require a priori assumptions, but unlike voxel-to-voxel analysis, it has the advantage of avoiding specific spatial confounds like residual head motion. However, it has the disadvantage of a somewhat arbitrary process of decomposing the neuroimaging data into statistically independent components as there is no best single model for multiple interconnected neurophysiological systems.[113]See Figure 8 for an overview of

some of the different methods of fMRI functional connectivity analysis.

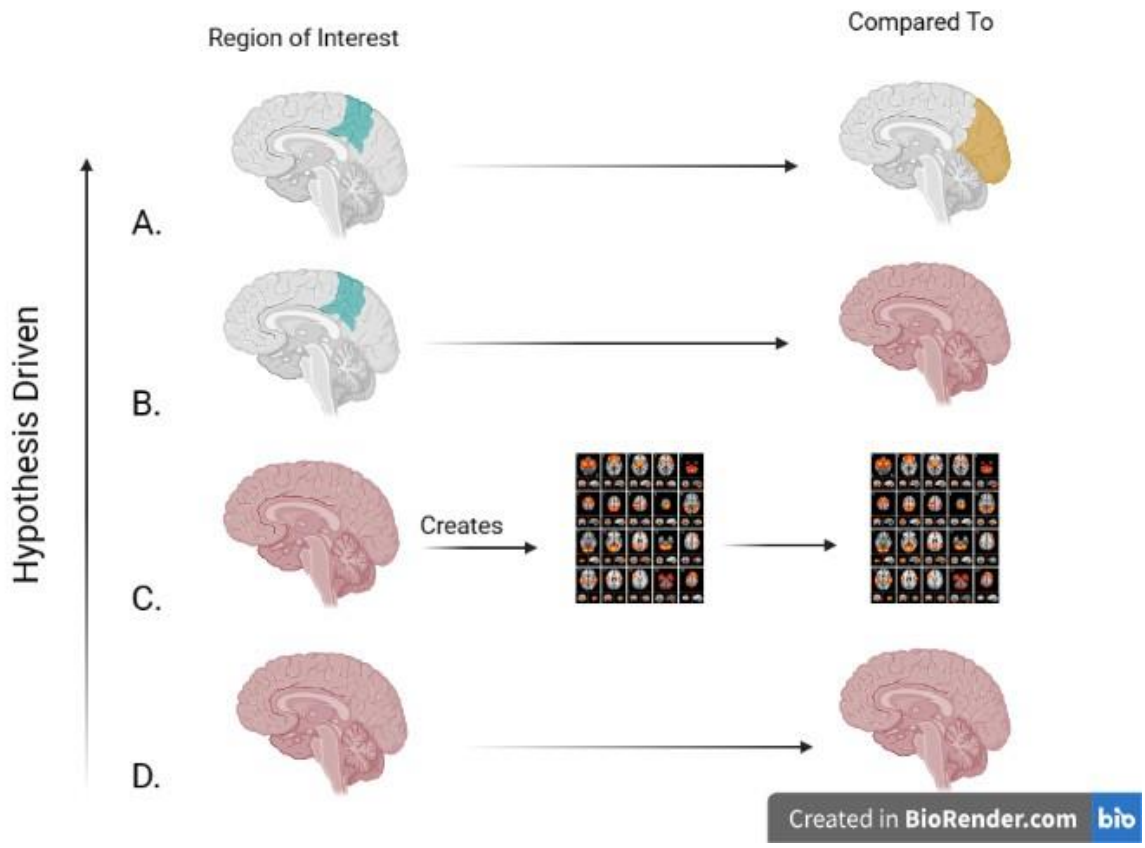


Figure 8. Overview of Various Methods of fMRI Functional Connectivity Analysis: **A)** Seed-to-seed functional connectivity analysis is the most hypothesis driven and least encompassing as it compares the temporal changes in the fMRI BOLD signal between the two seeds. **B)** Seed-to-voxel analysis compares changes in the BOLD signal in a seed to voxels in the whole brain. **C)** Independent component analysis creates and differentiates resting state networks from the fMRI BOLD signal from whole-brain analysis and then compares BOLD signal changes within and between the identified networks. **D)** Voxel-to-voxel intrinsic connectivity analysis is the most encompassing and least hypothesis driven as it analyzes changes in BOLD signal in voxel clusters under specific significance thresholds. Created in BioRender.

2.3.2 Pseudo-Continuous Arterial Spin Labeling

pCASL is another non-invasive functional imaging method that measures cerebral blood flow. The temporal resolution of pCASL is 1-3 seconds, while the spatial resolution is around 2-4mm in plane and

4-8mm slice thickness. This means that typically pCASL has a lower temporal and spatial resolution than fMRI. Despite these drawbacks, pCASL has a significant advantage in that it can measure cerebral blood flow (CBF) directly, while fMRI measures CBF indirectly through changes in blood oxygenation levels.

To measure CBF, pCASL uses a radiofrequency pulse to invert the magnetization of arterial blood water of hydrogen protons. This inversion occurs at the neck or base of the skull in order to view the flow of the arterial blood through the brain vasculature. What differentiates pCASL from other forms of arterial spin labeling, is that the radiofrequency pulse is delivered in a train of short pulses over an extended labeling period, with the labeling period being divided into delivery of radiofrequency pulses and image acquisition. This minimizes the magnetization transfer of hydrogen inversion from labeled arterial blood water to unlabeled arterial blood water already located in the brain vasculature that confounds the ASL signal and is more pronounced in a continuous spin labeling paradigm. Pseudo-continuous also maintains the higher signal-to-noise ratio of continuous spin labeling than a pulse arterial spin labeling paradigm.[114]

After labeling the arterial blood water, there is a post-labeling delay in which the labeled blood water protons continue to flow into the brain and exchange with the tissue water protons. After the post-labeling delay, MRI images are acquired during the period when the labeled blood water is perfusing into the tissue. These images are referred to as the labeled images, as they capture the signal from the labeled blood water that has mixed with the tissue water.

Subsequently there is a further delay that allows the labeled protons to be washed away and exchanged with unlabeled water. This is when the control MRI images are taken to calculate the perfusion image. The perfusion image is calculated by subtracting the labeled images from the controlled ones (see Figure 9 for an overview of the basic principles of arterial spin labeling).

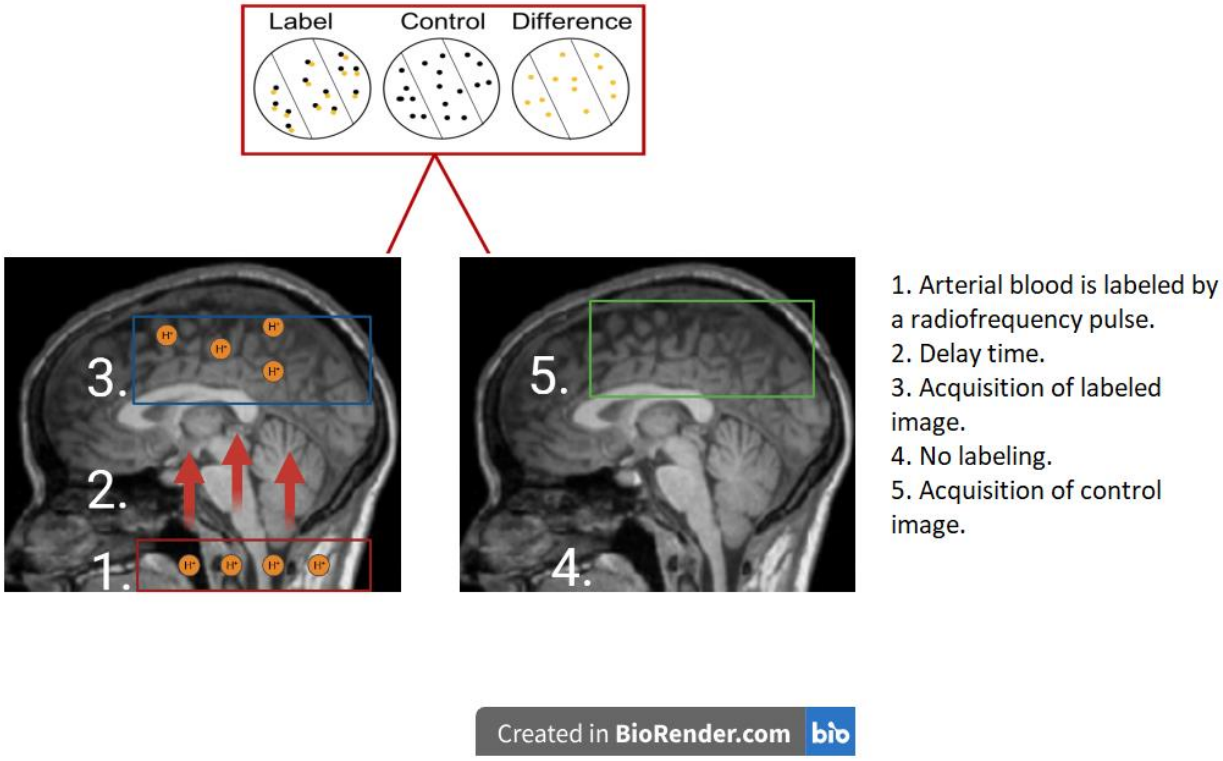


Figure 9. Overview of the Steps of Arterial Spin Labeling*:* Arterial blood is labeled by radiofrequency pulse before it enters the brain vasculature. Then there is a delay time to allow for the labeled hydrogen atoms to perfuse into brain tissue of interest. A labeled image is taken after this delay time. A second control image is taken after allowing for adequate time for the labeled hydrogen atoms to disperse from the brain tissue of interest. The perfusion image is then calculated by subtracting the labeled images from the control ones (Adopted from Alhindi, 2018).[115] Created in BioRender.

2.3.3 Transcranial Direct Current Stimulation, the Dorsolateral Prefrontal Cortex and Neuroimaging

In terms of tDCS and fMRI analysis for the DLPFC, there have been some findings on the effects of tDCS on wider resting-state networks[19,99,116,117], but with some differences in methodology and results. All studies except one found that anodal tDCS targeting the DLPFC increased functional connectivity in the central executive network. The one exception found that tDCS to the left DLPFC caused a decrease in the functional connectivity between the frontoparietal network and the ACC, while simultaneously causing

an increase of connectivity between the ACC and the orbitofrontal network.[117] A possible explanation for this difference in result is that it was the only study to place the cathode on the contralateral ventromedial PFC, which likely changed the flow of the current. Two of the four studies also found that applying tDCS to the DLPFC resulted in a decrease of connectivity for the DMN[19,116], with one of the four finding an increase of DMN connectivity from DLPFC stimulation.[99] Overall, these studies highlight that the DLPFC is a region highly interconnected within the central executive network, and that anodal tDCS stimulation can modulate the activity of the central executive network and the DMN, however, differences in methodologies and results make findings between studies difficult to compare.

pCASL analysis has yielded significant findings regarding the impact of targeting the DLPFC with tDCS, demonstrating widespread functional changes distant from the intended site. Anodal tDCS applied to the DLPFC resulted in increased cerebral blood flow (CBF) in the thalamus, lateral prefrontal cortex, midcingulate cortex, and paracingulate cortex, as observed in previous studies[101,118] and conversely, cathodal tDCS applied to the DLPFC led to a decrease in CBF in the thalamus and temporal gyrus.[118] It is worth noting that the DLPFC and thalamus exhibit robust structural and functional interconnections, as highlighted by previous research.[119,120] Consequently, the general outcomes of these investigations indicate that tDCS targeting the DLPFC can modulate the functional connectivity between the DLPFC and thalamus. Moreover, the midcingulate cortex, paracingulate cortex, and DLPFC are closely associated brain regions involved in various cognitive processes, including cognitive control[121] and emotion regulation.[122,123] Hence, it is unsurprising that targeting the DLPFC elicits CBF changes in these regions. Another study demonstrated that left DLPFC stimulation through tDCS not only increased CBF in the target area but also in the adjacent ACC[124], which, as mentioned earlier, is implicated in executive functions alongside the DLPFC. [84] In summary, these pCASL tDCS DLPFC studies unequivocally illustrate the strong interconnectedness of the DLPFC with the thalamus and other executive function regions.

Furthermore, they elucidate that tDCS applied to the DLPFC can elicit CBF changes in regions beyond the immediate target area.

PET is a functional neuroimaging technique that uses the injection of a radioactive tracer. Some of the most common tracers are fluorodeoxyglucose, which is used to assess glucose metabolism, and ^{11}C-raclopride which is used to assess dopamine receptor availability. The radioactive isotope attached to the metabolic molecule emits positrons which are annihilated when they collide with electrons, and this releases gamma rays that can be detected and used to construct a functional image.[125]

One of the most common uses of PET for investigating the neurophysiological mechanisms of tDCS for the DLPFC is to measure its effects on dopamine release.[102,126,127] These studies have shown that with the anode targeting the left DLPFC and the cathode contralaterally on the right, the application of tDCS can lead to an increase of dopamine release from the ventral striatum. Although the mechanism of how tDCS causes this increased release of dopamine is not fully elucidated, it is still highly suggestive that the DLPFC has significant direct or indirect connections to the nigrostriatal dopamine pathway and can modulate its function.

EEG measures and amplifies the electric signals produced via brain activity. It has an advantage over PET and fMRI in its temporal resolution as it can measure the electric signals of neuronal firing directly instead of the indirect changes in CBF or other metabolic markers that follow an action potential. However, the spatial resolution is much weaker making it difficult to find significant results when measuring an area as small as the DLPFC.[128] Therefore, most results of DLPFC tDCS on the EEG signal are reported more broadly on its effects to the prefrontal region. Studies have shown that applying tDCS to the DLPFC enhanced neural oscillatory markers of cognitive control[129] and consciousness[130] as well as increased activity in the ACC and medial frontal cortex.[131] These studies

provide further evidence that the DLPFC is involved in executive functions and engages nearby frontal regions. See table 1 for an overview of these studies of tDCS on the DLPFC.

Table 1. Summary of studies applying tDCS to the DLPFC

Authors	Target Region(s)	Montage	Duration	Intensity	Electrode Size	Functional Modality	General Findings
Peña-Gómez et al. 2012	Left/Right DLPFC	Anodal F3/Cathodal Right SO Anodal F4/Cathodal Left SO	20 minutes	2mA	$35cm^2$	fMRI	tDCS to the left and right DLPFC caused an increase of temporal synchronicity to the CEN and a spatial decrease to the DMN
Keeser et al. 2011	Left DLPFC	Anodal F3/ Cathodal Right SO	20 minutes	2mA	$35cm^2$	fMRI	tDCS to the left DLPFC caused an increase of coactivations in the DMN and left and right FPN
Soleimani et al. 2022	Right DLPC	Anode F4/Cathode F3	20 minutes	2mA	$35cm^2$	fMRI	tDCS to the right DLPFC caused an increase of FC to the CEN and a decrease of FC in the DMN
Leaver et al. 2022	Left DLPFC	Anode F3/ Cathode F8	5 minutes	2mA	$35cm^2$	fMRI	tDCS to the left DLPFC decreased FC for the FPN and increased FC for the OFN
Sacca et al. 2023	Right DLPFC	Anode F4/Cathode Left SO Cathode F4/Anode Left SO	20 minutes	2mA	$8cm^2$	pCASL	Anodal tDCS to the right DLPFC increases CBF in thalamus, while cathodal tDCS increased CBF in the PFC
Jog et al. 2021	Left DLPFC	Anode F3/ Cathode F8	20 minutes	2mA	$35cm^2$	pCASL	Anodal tDCS to the left DLPFC caused an increase of CBF in the left DLPFC
Stagg et al. 2013	Left DLPFC	Anode F3/ Cathode Right SO Cathode F3/ Anode Right SO	20 minutes	1mA	$35cm^2$	pCASL	Anodal tDCS to the left DLPFC caused an increase of CBF for left MCC and ParaCG. Cathodal tDCS to the left DLPFC caused a decrease of CBF in thalamus

Table 1. Continued

Authors	Target Region(s)	Montage	Duration	Intensity	Electrode Size	Functional Modality	General Findings
Bunai et al. 2021	Left DLPFC	Anode F3/Cathode F4	2x13 minutes	2mA	35cm^2	PET	Anodal tDCS to the left DLPFC caused an increase of GABA in the left striatum and a decrease in the right
Fukai et al. 2019	Left DLPFC	Anode F3/Cathode F4	2x13 minutes	2mA	35cm^2	PET	Anodal tDCS to the left DLPFC caused an increase of dopamine release in the right ventral striatum
Fonteneau et al. 2018	Left DLPFC	Anode F3/Cathode F4	20 minutes	2mA	35cm^2	PET	Anodal tDCS to the left DLPFC caused an increase of dopamine release in the striatum
Boudewyn et al. 2018	Left DLPFC	Anode F3/ Cathode Right SO	20 minutes	2mA	35cm^2	EEG	Anodal tDCS to the left DLPFC increased high frequency gamma bands associated with proactive control + increased performance on control task
Hermann et al. 2020	Left DLPFC	Anode F3/ Cathode Right SO	20 minutes	2mA	25cm^2	EEG	Anodal tDCS to the left DLPFC increased FC and power of the theta-alpha band that are associated with consciousness
Keeser et al. 2011	Left DLPFC	Anode F3/ Cathode Right SO	20 minutes	2mA		EEG	Anodal tDCS to the left DLPFC decreased delta bands and increased activity in the ACC and MFC

Key: MFC, Middle Frontal Cortex; ACC, Anterior Cingulate Cortex; SO, Supraorbital Area; CEN, Central Executive Network; FPN, Frontoparietal Network; OFN, Orbitofrontal Network; PFC, Prefrontal Cortex; MCC, Midcingulate Cortex; ParaCG, Paracingulate Cortex; FC, Functional Connectivity

3. Aim, Objectives, and Hypothesis

Most studies investigating the underlaying mechanisms of tDCS are based on studies stimulating the motor cortex. This is an issue because often those findings are not transferable to other brain regions. For example, the prefrontal cortex is one of the most frequently targeted regions for many neuropsychiatric conditions, yet it is unclear how left vs. right prefrontal stimulation would produce the same or different results. Therefore, our overarching **aim** is to seek to further the understanding of the mechanisms of tDCS by investigating the different neurophysiological and behavioral effects of the tDCS when applied to the left vs. right dorsolateral prefrontal cortex (DLPFC). This aim will be addressed by three different objectives using different modalities to measure neurophysiological or behavioral function:

Objective 1) Identify how the application of tDCS to the right and left DLPFC effects functional connectivity using resting-state fMRI.

Objective 2) Identify if applying tDCS to the left and right DLPFC respectively causes any changes in Stroop interference score.

Objective 3) Identify how the application of tDCS to the right and left DLPFC effects cerebral blood flow using pCASL.

Our **hypothesis** is that due to the DLPFC being known as a hemispherically specialized region, the neurophysiological and behavioral effects of tDCS targeting the DLPFC will be hemispherically differentiated as well.

4. Methods

4.1 Study Participants

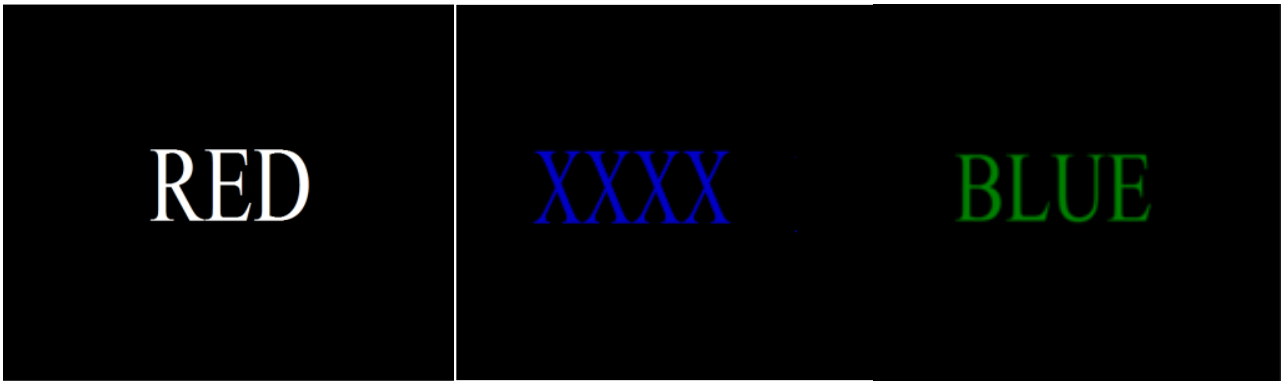
Thirty-nine participants (11 male, 28 female) were recruited for this study with a median age of 49.7±17 years. Participants were recruited from community at large. This study was approved by the Biomedical Research Ethics Board of the University of Manitoba and all participants provided written informed consent prior to participating. After recruitment, participants were then cognitively and behaviorally assessed with the Montreal Cognitive Assessment (MoCA)[132], Stroop test[133], and Beck-Depression Inventory II (BDI-II).[134]

Exclusion criteria for this study included: 1) Pregnant or breastfeeding women; 2) History of neurological or psychiatric disease; 3) Metal implants or pacemaker; 4) Abnormal MRI; 5) A Montreal Cognitive Assessment (MoCA) score lower than 25/30; 6) A Beck Depression Inventory II (BDI-II) score of 10 or above; 7) Severe hypertension; 8) Cardiovascular disease; 9) Family history of epilepsy.

4.2 Stroop Test Administration

Each participant took the Stroop test a total of two times: Once during the initial cognitive assessment, and once after the tDCS session (within 30 minutes). No practice trial was performed, but before initiating the Stroop test, the participants were given verbal instruction on how to execute the test. The Stroop test was administered via a computer using the automated neurophysiological assessments metrics (ANAM) program. The test is presented via three blocks (45 seconds per block). In the first block **a)** the words “Green”, “Red” and “Blue” are presented in white type and the subject must press a corresponding computer key for each word (Figure 10). For the second block **b)**, a series of XXXX’s is presented in either blue, red or green type and the subject must press a corresponding computer key for

the type colour. For the third block **c)** the words “Green”, “Red” and “Blue” are presented in incongruent type colours and the subject must press a corresponding computer key for the type colour.



A **B** **C**

***Figure 10. Stroop Test*: A)** neutral word task (first block) **B)** neutral colour task (second block) **C)** incongruent colour-word task (third block).

Stroop interference score was calculated using the method developed by Golden [133], in which interference score is equal to the number of correct responses for the third block (#CorrectLv3) minus the predicted performance for the third block. Predicted performance of the third block is calculated by multiplying the number of correct responses for blocks one (#CorrectLv1) and two (#CorrectLv2) and dividing it by the summation of correct responses for blocks one and two. This is summarized in the equation:

$$Stroop\ Interference\ Score = \#\ CorrectLv3 - \frac{[\#Correct\ Lv2 \times \#CorrectLv1]}{[\#Correct\ Lv2 + \#CorrectLv1]}$$

These Stroop interference score values were then standardized for sex and age by using the ANAM Stroop interference score database.[135]"The interpretation of the normalized Stroop interference score involves considering a performance of 100 as the average for an individual within a particular age and gender group, where a higher score indicates weaker inhibition performance, or in other words, greater interference. Score differences of 15 represent one standard deviation different from the mean.

4.3 Application of tDCS and Neuroimaging

After neuropsychological assessment, participants were randomly assigned to three different treatment groups: application of tDCS to the left DLPFC (Anode placement to F3 for the 10-20 international EEG placement standard); application of tDCS to the right DLPFC (Anode placement of F4); and the sham stimulation (Figure 11).

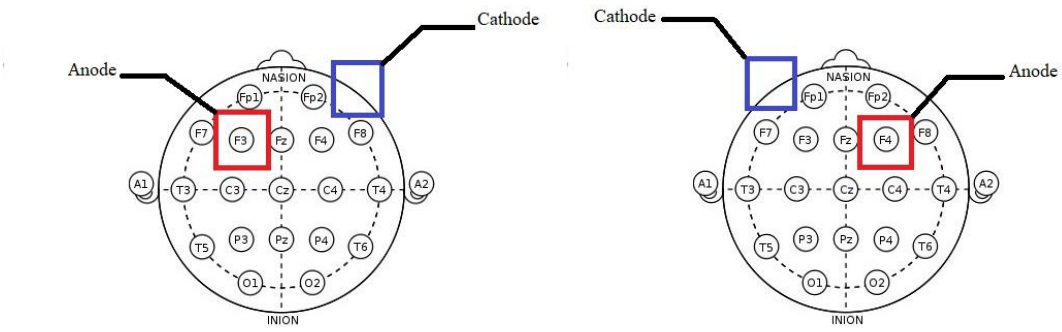


Figure 11. tDCS Target Location: 10-20 International EEG placement standard for tDCS targeting the left and right DLPFC respectively.

Stimulation was provided via a Soterix Medical 1x1 Transcranial Direct Current Low-Intensity Stimulator with a 5x7cm sponge at a current of 1.5mA. The sponges and connected carbon-rubber electrodes were placed on the participants head via an adjustable EASYstrap. For sham stimulation, the anode was placed either left or right (F3 or F4). For all groups the cathodal montage was placed on the contralateral supraorbital region. Both participants and researchers that applied tDCS were blinded to subject group placement.

All participants were scanned with 3T MRI (Siemens/IMRIS Verio) equipped with 12-channel head coil located at the Kleysen Institute for Advanced Medicine at the University of Manitoba. During scanning, participants were instructed to keep their eyes open and not to fall asleep. MRI sequence were: [Structural T1 (8 min), pCASL (5 min), pre-tDCS resting-state fMRI (11 min), tDCS (1.5 mA, 15 min), post-tDCS resting-state fMRI (11 min), post-tDCS pCASL (5 min)]. Between the pre- and post-tDCS fMRI scans subjects laid still in the scanner while tDCS was applied. For the sham condition the current was only applied for a 30 second ramp up and down.

The structural T1 image was acquired using an MPRAGE sequence with TR/TE/TI = 2300/3.02/900ms, 240 slices, flip angle = 9°, FOV = 256 mm x 256 mm, 1.0 mm^3 (isotropic) resolution. After structural imaging, resting state fMRI scans were collected using the following parameters: repetition time [TR] = 2000ms; echo time [TE] = 28 ms; flip angle = 77° slice thickness = 4 mm; field of view [FOV] = 220mm; voxel size = 3.4 X 3.4 X 4.0 mm; scan duration = 11 min.

The pCASL parameters were as follows: TR/TE = 4000/12, 20 slices, flip angle = 90°, FOV = 240 mm x 240 mm^2, 3.8 mm x 3.8 mm x 5.0 mm resolution, inter-slice space = 1 mm, labelling time = 2.0 s, post label delay time = 1.2 s, bandwidth = 3kHZ/pixel. For each participant, 45 label/control image pairs will be acquired.

4.4 Behavioral Data Analysis

Behavioral statistical analysis was conducted using IBM version 27 SPSS software. One-way ANOVA was used to compare the group (left, right, and sham stimulation) differences of age, MoCA, BDI-II, and pre-tDCS Stroop interference score. The group differences in sex and handedness were analyzed using a chi-square test. The effects of different tDCS applications (left, right, and sham) on Stroop interference scores were analyzed using a general linear model repeated measures. A significant interaction effect (group × time) was further analyzed by a post-hoc Bonferroni test. Age was included as a covariate and

sex as an additional between-subject factor within the model to see if these variables had any consequence on the effect of significance of the three treatment groups on Stroop interference score. Effect size for the treatment groups was calculated using partial eta squared. Outliers were identified for tDCS-induced changes in Stroop interference scores within each treatment group (i.e., being less than 1.5 Interquartile range (IQR) from Q1 or 1.5 IQR greater than Q3) for Δ interference, resulting in exclusion of three subjects from the left DLPFC stimulation group. While these individuals were excluded from the statistical analysis, we separately examined them qualitatively, and discussed the potential explanation in the discussion section.

4.5 fMRI Functional Connectivity Analysis

Standard preprocessing was applied to the resting state-fMRI data using the Functional Connectivity toolbox, CONN (*RRID:SCR_009550), release 18b).*[136] The first step of the pipeline is the realignment of the functional images in order to correct for any head motion artefacts. Next, a slice-timing correction was performed to correct for differences in time for the acquisition of slices in the fMRI acquisition. This was followed by coregistration of the participants functional and structural T1 scans. Segmentation of the anatomical images into cerebral spinal fluid (CSF), white matter and grey matter components and normalization of the functional data into a standard anatomical template in a common space then followed. The resulting image was then smoothed with a full width at height maximum 8x8x8mm Gaussian kernel. Denoising was applied via linear regression on CSF and white matter masks produced during segmentation. Finally, a band-pass filter of 0.008-0.09Hz was also applied to minimize the influence of physiological, head-motion and other noise sources.

To investigate any changes in functional connectivity from the DLPFC, first pre-defined seed regions were used. These pre-defined seed regions included the left and right superior frontal gyrus and mid frontal gyrus from the CONN ROI atlas, as well as the F3 and F4, which were defined by creating

8mm radius spheres at MNI coordinates -38, 34,47 and 39,35,48 respectively.[137] Therefore, to investigate each stimulation effects (left or right tDCS), six separate 2x2 factorial analyses (real vs. sham × pre vs. post) were performed with six different pre-defined ROIs as seeds.

While the seed-based connectivity analysis can reveal function connectivity changes associated with the pre-defined seeds, it is probable that the "hotspot" of tDCS effect does not perfectly overlap with those a priori region-of-interests [42] which then can dilute the true effects. To locate the exact hotspots of tDCS, we performed voxel-to-voxel IC analysis. The voxel-to-voxel IC measures the node centrality of each voxel and defines a voxels centrality by the strength of its connectivity to the rest of the voxels in whole brain. Mathematically, this is defined as root mean square of correlation coefficients between a specific voxel and all other brain voxels. For our IC analysis, we performed two sets of 2×2 factorial analyses between groups (real vs. sham) and time (pre- vs. post-tDCS) for each left and right tDCS, separately.

Significant clusters found in the intrinsic connectivity voxel-to-voxel analysis were then imported as masks into CONN to be used a ROIs for seed-to-voxel analysis following the same pipeline and procedures as the previous seed-to-voxel and voxel-to-voxel analysis.

For all fMRI functional connectivity image analyses, we used the statistical threshold for a voxel to belong to a cluster at $p < 0.001$ (uncorrected), while cluster extent threshold was $p < 0.05$ (false-discovery-rate corrected). Age and sex were also included as second level covariates for seed-to-voxel and voxel-to-voxel analysis.

4.6 pCASL Cerebral Blood Flow Analysis

pCASL analysis was conducted via the arterial spin labeling toolbox (ASLtbx; https://www.cfn.upenn.edu/~zewang/ASLtbx.php). The default pipeline was used which consists of the steps of motion correction, co-registration of pCASL and structural MRI, spatial smoothing, brain mask

creation and finally CBF quantification.[138] After the CBF images were created by the ASLtbx, SPM12 was used for the co-registration of CBF images and T1 structural MRI, spatial normalization by wrapping to Montreal neurological institute (MNI) standard space, and finally spatial smoothing using an 8x8x8mm Gaussian kernel.

Changes in mean CBF were then analyzed on a voxel-whole-brain level and specifically in the F3/F4 and CONN atlas ROIs which were used as inclusive masks. These changes in mean CBF were then compared to tDCS treatment via a 3×2 factorial analysis which examined the interaction effects between stimulation condition (left, right, and sham) and time (pre- vs. post-tDCS). Voxel-based analysis was also performed for changes of CBF maps. The statistical threshold for a voxel to belong to a cluster was $p<0.001$ (uncorrected), while cluster extent threshold was $q<0.05$ (false-discovery-rate corrected).

5. Results

5.1 Demographic Analysis

Relevant demographic data of the participants are included in Table 2. No significant differences across the treatment groups (left, right, and sham tDCS) were found in the age (p=0.488), sex (p=0.860), handedness (p=0.549), MoCA (p=0.293), pre-tDCS Stroop interference score (p=0.424) or BDI-II (p=0.268) scores of the participants.

Table 2. Demographic information for participants

Parameters	Treatment Group			Significance
	Left tDCS	Right tDCS	Sham	(p)
Number of Subjects (M:F)	12(4:8)	14(4:10)	13(3:10)	0.860
Age	47.3±4.6	54.1±4.3	47.2±5.4	0.488
Handedness (L:R:A)	(0:12:0)	(1:13:0)	(1:11:1)	0.549
MoCA	28.4±0.33	28±0.60	27.4±0.31	0.293
BDI-II	3.0±0.78	4.1±0.97	2.2±0.69	0.268

Key: L:R:A, left right ambidextrous; MoCA Montreal cognitive assessment; BDI-II, Beck Depression Inventory II. Significance measures the differences of sex, age, handedness etc. between the three treatment groups.

5.2 tDCS Effects on Interference Score

A significant interaction effect was found between treatment (left, right vs. sham tDCS) and time (pre vs. post tDCS) ($F(2,33)=3.68$, p=0.037; Figure 12). For treatment groups, tDCS to the right DLPFC significantly decreased Stroop test interference score post-tDCS stimulation compared to pre-tDCS stimulation (p<0.001, post-hoc Bonferroni tests), but the application of tDCS in the left (p=0.976) or sham conditions (p=0.172) had no significant effect on interferences score in the comparison of pre- and post-tDCS time

periods. Effect size of the left and right compared to the sham treatment groups were η_p^2 = 0.336 and 0.056 respectively. When included as a covariate, age (p=0.587) or sex (p=0.863) did not have any significant effects.

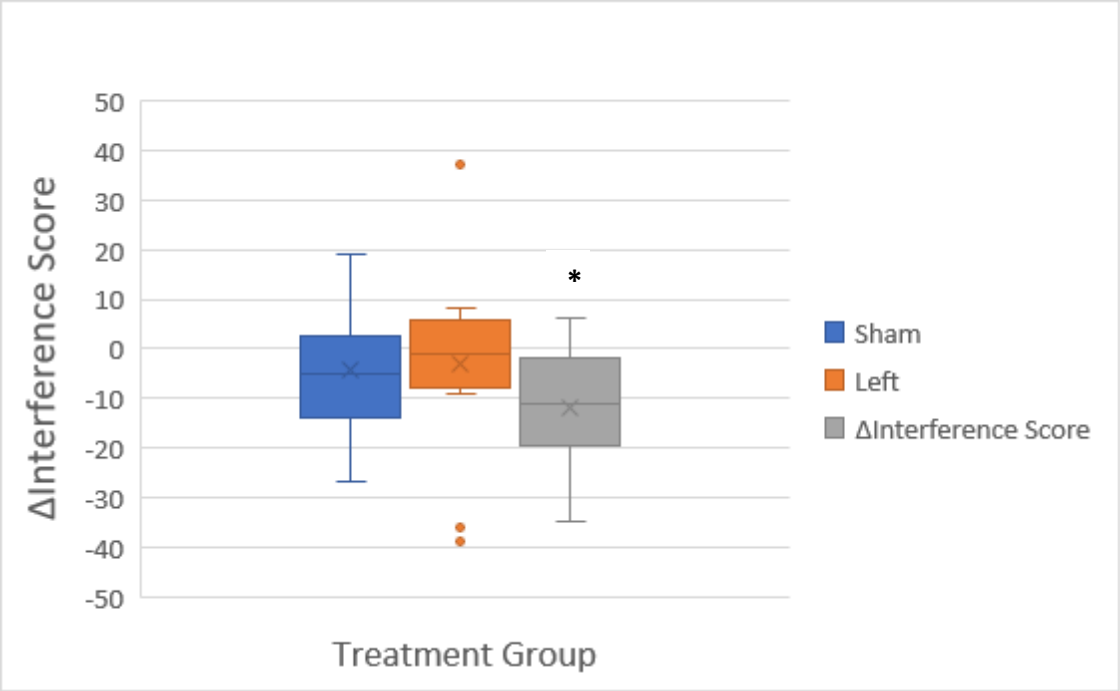


Figure 12. ΔInterference Score Post vs. Pre tDCS **:** Change in Stroop test interference score for post vs. pre tDCS in different treatment groups (sham, left, and right DLPFC). Stroop interference score is a normalized value, with a performance of 100 being the mean for an individual of a specific age group and a higher score representing poorer inhibition performance. Outliers (filled circles) were identified by being 1.5 inclusive interquartile range from below the first quartile or above the third quartile and were excluded in the statistical analysis. Significant effect of the treatment group was identified (F(2,33)=3.68, p=0.037). *p<0.001 by post-hoc Bonferroni tests.

5.3 Functional Connectivity Analysis with A Priori Regions of Interest

Seed-to-voxel functional connectivity analyses with a priori region of interests (i.e., the left and right superior frontal gyrus and mid frontal gyrus from the CONN ROI atlas, as well as the F3 and F4 at MNI coordinates x=-38, y=34, z=47 and x=39, y=35, z=48) did not reveal any significant clusters for an interaction effect (real (left or right) vs. sham × post- vs. pre-tDCS).

5.4 Voxel-to-Voxel Intrinsic Functional Connectivity Analysis

To locate the primarily affected brain regions by tDCS which may not be confined to the pre-defined regions of interests (i.e., superior frontal gyrus (SFG), middle frontal gyrus (MFG), and F3/F4) voxel-to-voxel IC analyses were performed.

A 3x2 analysis for any difference between the three treatment groups (sham, left and right tDCS) and time (pre- and post -tDCS) found a cluster located at the frontal pole (p=0.018 cluster-level FDR-corrected, p<0.001 peak-level uncorrected, peak MNI coordinates +32,+52,+08). Further one-way ANOVA analysis of this cluster revealed that right tDCS caused a decrease in the frontal pole of a significant mean difference in comparison to the sham (p<0.001) and left (p=0.001) treatment groups, with treatment group having a partial eta squared effect size of $\eta_p^2 = 0.624$.

The results of our 2x2 analysis are summarized in Table 3. As hypothesized, the left DLPFC stimulation increased IC in the left prefrontal region (p=0.008 cluster-level FDR-corrected, p<0.001 peak-level uncorrected) with peak coordinates located at the middle frontal gyrus (x=-48, y=+12, z=+46; figure 13A). It also caused a increased IC in the postcentral and precentral gyrus (p=0.023 cluster-level FDR-corrected, p<0.001 peak-level uncorrected) located at peak coordinates (x=+38 y=-24, z=+46) and decreased IC in three different clusters located near the left precuneus cortex (x=-02, y=-54, z=+58, p=0.043 cluster-level FDR-corrected, p<0.001 peak-level uncorrected), left fusiform gyrus (x=-30, y=-44, z=-08, p=0.008 cluster-level FDR-corrected, p<0.001 peak-level uncorrected) and left cerebellum (x=-08, y=-38, z=-20, p=0.007 cluster-level FDR-corrected, p<0.001 peak-level uncorrected). Contrarily, tDCS to the right DLPFC decreased IC in the right prefrontal cortex (p=0.008, cluster-level FDR-corrected, p<0.001 peak-level uncorrected) at peak coordinates (x=+30, y=+52, z=+8; figure 13B) near the right frontal pole, replicating our result from the 2x2 analysis. Inclusion of covariates (sex and/or age) did not change the results significantly.

Table 3. Summary of fMRI IC results

Cluster Region	BA	Laterality	IC Change	KE	p(FDR)	Peak Voxel			
						T-Value	X	Y	Z
Left vs. sham tDCS									
1 Precuneus Cortex	7		Decrease	40	0.043	-4.63	-2	-54	58
2 Middle Frontal Gyrus	8/6	Left	Increase	67	0.008	8.09	-48	12	46
3 Temporal fusiform Cortex	37	Left	Decrease	69	0.008	-5.99	-30	-44	-8
Temporal Occipital Cortex	37	Left							
Lingual/Parahippocampal Gyrus	37	Left							
4 Cerebellum/Vermis		Left	Decrease	84	0.007	-6.45	-8	-38	-20
5. Postcentral Gyrus		Right	Increase	50	0.023	5.10	38	-24	46
Precentral Gyrus		Right							
Right vs. sham tDCS									
1 Frontal Pole	10	Right	Decrease	62	0.008	-6.36	30	52	8

Key: BA, Brodmann area; IC, intrinsic connectivity; KE, cluster extent; FDR, false-discovery-rate.

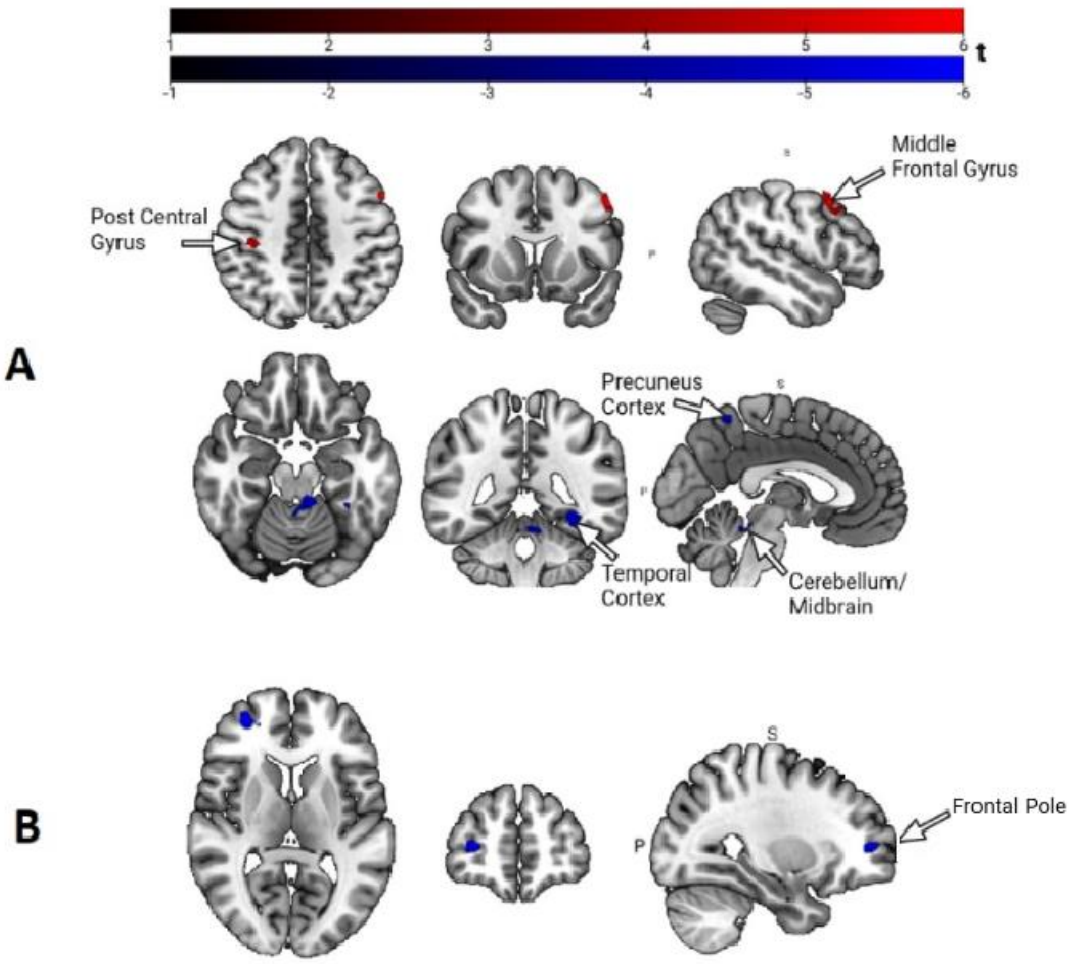


Figure 13. Changes in IC Following the tDCS: **A)**. Increased IC was identified in the left middle frontal gyrus after the left tDCS vs. sham (p<0.001 peak-level uncorrected; p=0.008 cluster-level FDR-corrected, peak MNI coordinates -48, +12, +46) and the post-central gyrus (p<0.001 peak-level uncorrected; p=0.023 cluster-level FDR-corrected, peak MNI coordinates +38,-24,+46; *top row*) . Decreased IC was observed in three different clusters located at the cerebellum/midbrain (p<0.001 peak-level uncorrected; p=0.007 cluster-level FDR corrected, peak MNI coordinates -08, -38, -20), temporal cortex (p<0.001 peak-level uncorrected; p=0.008 cluster-level FDR corrected, peak MNI coordinates -30, -44, -08) and precuneus cortex (p<0.001 peak-level uncorrected; p=0.043 cluster-level FDR corrected, peak MNI coordinates -02, -54, +58; *middle row*). **B)** Decreased IC was observed in the right prefrontal region after the application of tDCS to the right DLPFC (p<0.001 peak-level uncorrected; p= 0.008, cluster-level FDR-corrected, peak MNI coordinates +30, +52, +8).

5.4.1 Functional Connectivity Analysis with Intrinsic Connectivity Clusters

The significant clusters found from the voxel-to-voxel intrinsic connectivity analysis where then used as seed regions for seed-to-voxel whole brain analysis. No significant results were found.

5.5 pCASL Cerebral Blood Flow Analysis

No significant changes in CBF were found in the whole-brain voxel-based analysis or in any of the ROIs, i.e., seeds that were used in the functional connectivity analysis, F3 and F4, as well as the clusters identified from the voxel-to-voxel intrinsic connectivity analyses.

6. Discussion

The most intriguing finding of the present study was that the same anodal tDCS had opposite neurophysiological consequences (measured by fMRI-based IC) when it was applied to the left vs. right DLPFC compared to the sham stimulation (Figure 13). More specifically, applying tDCS to the left DLPFC caused an increase in the IC of a cluster of voxels at the ipsilateral middle frontal gyrus near the target site (24mm away from the approximated F3 coordinates), while applying tDCS to the right DLPFC caused a decrease in the IC of voxels near the ipsilateral frontal pole (44mm away from the approximated F4 coordinates). This neurophysiological discrepancy between left vs. right DLPFC stimulation effect was in line with the behavioral effects measured by Stroop test (Figure 12). The opposite effects of left vs. right DLPFC stimulation has previously been reported in motor sequence learning [139], negative imaging-invoked pupil dilation (potentially representing cognitive resource allocation) [6], and gaze disengagement from emotional faces .[140] To our knowledge, this is the first tDCS study where an opposite pattern of neurophysiological response (increased vs. decreased IC) was observed between left vs. right DLPFC stimulation.

One possible explanation for the asymmetric changes in IC due to tDCS is that the morphological differences between left vs. right DLPFC regions [141] could affect the direction of membrane potential changes induced by tDCS. Simulation studies have suggested that the direction of polarization (depolarization vs. hyperpolarization) can be influenced by the orientation of neurons. [14,142] For example, the tDCS-induced current flow can be opposite between the opposite sides of sulcal walls, and thus the direction of membrane potential changes can also be opposite, which determines the changes in neuronal excitability and subsequent changes to the BOLD signal and IC .[143]

Another possible explanation is the asymmetric distribution of neurotransmitters for the left and right DLPFC. Post-mortem studies have found significant hemispherical differences in the

distribution of neurotransmitters such as GABA and dopamine [144], however to our knowledge little has been done to investigate neurotransmitter differences between the hemispheres of the DLPFC. Previously, we have demonstrated that applying the same inhibitory rTMS to the left vs. right DLPFC differently modulates the task-induced striatal dopamine release.[15] Together, the present study result suggests that an extreme caution should be exercised when one designs a tDCS experiment targeting brain areas other than primary motor cortex where changes in neuroexcitability cannot be empirically tested with TMS-induced motor evoked potentials. Employing a neuroimaging technique can help determine the direction of physiological changes induced by the given tDCS parameters.

Of note, no significant results for an interaction effect were found for the seed-to-voxel based analysis using the predefined seeds, i.e., F3/F4-centered spherical volumes of interests, and the superior and middle frontal gyrus in the CONN atlas. One possible explanation for this negative result is that the 'hotspot' of the application of tDCS to F3 and F4 is not interchangeable with either of these seed regions. Many studies have shown that the peak electric field is not necessarily directly underneath the electrode.[145-147] Indeed, the voxel-to-voxel IC analysis localized the "hotspot" of tDCS effects to be 24-44mm away from the center of F3 and F4 projected locations. The IC-based hotspot fell on the left middle frontal gyrus (one of the pre-defined seeds), but they are significantly different in sizes (50 vs. 23430 voxels). Therefore, using the entire left middle frontal gyrus as a seed is not specific enough to elucidate the significant changes in functional connectivity induced by tDCS.

For the left DLPFC stimulation, in addition to the cluster of increased IC located in the middle frontal gyrus, there were three clusters of decreased IC located at the precuneus cortex, temporal cortex and cerebellum/midbrain. The temporal cortex and the precuneus cortex are known to be associated with the default mode network (DMN)[148,149], while the DLPFC is known be associated with the central executive network, which is anticorrelated to the DMN.[150] Therefore, increasing the dominance (i.e., IC) of the DLPFC in the overall brain networks may have resulted in decreased IC in the regions

included in DMN. The cerebellar contribution to the overall brain network configuration may have similarly been reduced by coincident IC increases in the DLPFC. It should be noted that recent studies have established that the cerebellum closely interacts with prefronto-parietal network and high-level cognitive functions while earlier neuroimaging studies have unjustifiably paid less attention to the cerebellum.[151]

Despite finding significant clusters in voxel-to-voxel analysis, when those clusters were used as seed regions in seed-to-voxel whole brain analysis, we did not find any significant results. We propose two possibilities for this finding. First, seed-to-voxel analysis involves averaging brain activity across multiple voxels within the seed region, which often requires a larger sample size to achieve sufficient statistical power compared to voxel-to-voxel analysis, where each voxel is treated as an independent data point. Second, the relatively low sample size of our treatment groups (12 left tDCS, 14 right, 13 sham) may be small enough for the inter variability of our participants anatomical features to affect the significance of the results when analyzing the clusters as seed regions.

No significant results were also found for pCASL analysis for the whole-brain and ROI based analyses. One possible reason for this null result is that pCASL has a lower signal to noise ratio and lower spatial resolution than fMRI. This lower spatial resolution may be of significant concern for analyzing the changes of CBF due to the application of tDCS on the DLPFC, especially if those effects are small and dispersed from the target site by causing functional connectivity changes to wider-brain networks.[152,153] For the null results for the ROI based pCASL analysis, previously mentioned weakness in seed-to-voxel analysis such as requirements for larger sample sizes for significance and being more susceptible to inter subject variability may also additionally apply. It is then not entirely surprising that ROI based pCASL analysis would also not find significant results using the same seed-regions as the seed-to-voxel fMRI analysis, which also did not find significant results using these seeds.

The lateral discrepancy of neuroimaging findings is in line with behavioral observation that only the right DLPFC stimulation improved the response time in Stroop test but not the left DLPFC stimulation. The improved Stroop test performance after the right DLPFC stimulation has previously been reported.[154,155] It has been hypothesized that this behavioral improvement is due to an increased ability of sustained attention and proactive inhibitory control in right DLPFC, which has been supported by other studies where it has been demonstrated that the right DLPFC is involved with error awareness [156] and monitoring of working memory.[157] It is yet unclear why this improvement in inhibition control was coupled with a decrease in IC in the right frontal pole. Of note, a lesion study on the frontal pole of macaques found that it led to an improvement in conflict and distraction management for a Wisconsin Card Sorting Test.[158] It is also possible that the decreased IC was a secondary remote effect of F4 stimulation which was 44mm away. Nevertheless, it should be noted that the size of the sponge electrodes was 5x7cm, and the cathodal end was placed on the contralateral supraorbital regions. Therefore, the current flow would have likely passed through the frontal pole region.

Although there were clear IC changes after the left DLPFC stimulation, no significant effect was observed in Stroop task performance. A few previous tDCS studies targeting the left DLPFC have also observed non-significant effects in Stroop interference score.[7,90,159,160] It is possible that the left DLPFC is already fully engaged in Stroop test at baseline and thus its increased IC (or its function) does not translate into better performance (i.e., ceiling effects). It should be cautioned that there were three outliers whose Stroop interference score was outside of 1.5 SD of the mean thereby excluded from the statistical analysis. Although the inclusion of these outliers does not change the significance of findings, it potentially suggests that the individual responses were more variable after the left DLPFC stimulation than the right DLPFC and sham stimulation.

7. Limitations and Future Directions

One significant limitation in our study is a small sample size between the treatment groups (12 left tDCS, 14 right, 13 sham). This smaller sample size may have limited our ability to find significant findings in the seed-based fMRI and pCASL analysis.

Another limitation of our study is that the seed regions could perhaps be better defined. We previously stated that our null results may be due to the effects of tDCS not being located at the electrode[33], so creating a 8mm radius sphere around the electrode placements is a simple, yet crude ROI definition. A more refined ROI could be created by constructing and validating a realistic head model through a technique like fine element modeling (FEM).

In FEM, the MRI scans are used to obtain data on the geometry, anatomy, and mechanical properties of biological tissues of interest. This data is then used as input to create a computer-generated 3D model of the tissue, which is divided into finite elements, typically tetrahedral or hexahedral elements, to represent the discretized regions of interest. Each finite element has its own properties, such as material properties, shape, and location, and the interactions between these elements are mathematically modeled based on the governing equations of mechanics, such as the linear elasticity or nonlinear viscoelasticity equations.[161]

Creating and validating a FEM model would allow us to create a seed region based on the electric field distribution in brain tissue from tDCS, increasing precision of our ROI. High definition tDCS could also be investigated to further increase the precision of the application of tDCS currents for better seed-based analyses.

8. Conclusion

To our knowledge, we showed for the first time that the same anodal tDCS application to the left vs. right DLPFC resulted in opposite neurophysiological changes in the targeted areas assessed by resting-state IC (increased vs. decreased, respectively). Caution should therefore be observed when extrapolating the findings from motor cortex stimulation, i.e., anodal tDCS increases neuronal excitability while cathodal tDCS decreases it to those of prefrontal regions. Our study also provides further evidence that tDCS to the left DLPFC does not increase performance for Stroop interference, while also highlighting that the right DLPFC may be more involved with incongruent stimuli.

References

1. Lefaucheur JP, Antal A, Ayache SS, et al. Evidence-based guidelines on the therapeutic use of transcranial direct current stimulation (tDCS). *Clin Neurophysiol*. Jan 2017;128(1):56-92. doi:10.1016/j.clinph.2016.10.087
2. Priori A, Berardelli A, Rona S, Accornero N, Manfredi M. Polarization of the human motor cortex through the scalp. *Neuroreport*. Jul 13 1998;9(10):2257-60. doi:10.1097/00001756-199807130-00020
3. Nitsche MA, Paulus W. Excitability changes induced in the human motor cortex by weak transcranial direct current stimulation. *J Physiol*. Sep 15 2000;527 Pt 3(Pt 3):633-9. doi:10.1111/j.1469-7793.2000.t01-1-00633.x
4. Mordillo-Mateos L, Turpin-Fenoll L, Millán-Pascual J, et al. Effects of simultaneous bilateral tDCS of the human motor cortex. *Brain Stimul*. Jul 2012;5(3):214-222. doi:10.1016/j.brs.2011.05.001
5. Lang N, Nitsche MA, Paulus W, Rothwell JC, Lemon RN. Effects of transcranial direct current stimulation over the human motor cortex on corticospinal and transcallosal excitability. *Exp Brain Res*. Jun 2004;156(4):439-43. doi:10.1007/s00221-003-1800-2
6. Allaert J, Sanchez-Lopez A, De Raedt R, Baeken C, Vanderhasselt MA. Inverse effects of tDCS over the left versus right DLPC on emotional processing: A pupillometry study. *PLoS One*. 2019;14(6):e0218327. doi:10.1371/journal.pone.0218327
7. Baumert A, Buchholz N, Zinkernagel A, et al. Causal underpinnings of working memory and Stroop interference control: Testing the effects of anodal and cathodal tDCS over the left DLPFC. *Cogn Affect Behav Neurosci*. Feb 2020;20(1):34-48. doi:10.3758/s13415-019-00726-y
8. Dubreuil-Vall L, Chau P, Ruffini G, Widge AS, Camprodon JA. tDCS to the left DLPFC modulates cognitive and physiological correlates of executive function in a state-dependent manner. *Brain Stimul*. 2019;12(6):1456-1463. doi:10.1016/j.brs.2019.06.006
9. Smirni D, Turriziani P, Mangano GR, Cipolotti L, Oliveri M. Modulating Memory Performance in Healthy Subjects with Transcranial Direct Current Stimulation Over the Right Dorsolateral Prefrontal Cortex. *PLoS One*. 2015;10(12):e0144838. doi:10.1371/journal.pone.0144838
10. Heinze K, Ruh N, Nitschke K, et al. Transcranial direct current stimulation over left and right DLPFC: Lateralized effects on planning performance and related eye movements. *Biol Psychol*. Oct 2014;102:130-40. doi:10.1016/j.biopsycho.2014.07.019
11. Brunelin J, Mondino M, Gassab L, et al. Examining transcranial direct-current stimulation (tDCS) as a treatment for hallucinations in schizophrenia. *Am J Psychiatry*. Jul 2012;169(7):719-24. doi:10.1176/appi.ajp.2012.11071091
12. Palm U, Schiller C, Fintescu Z, et al. Transcranial direct current stimulation in treatment resistant depression: a randomized double-blind, placebo-controlled study. *Brain Stimul*. Jul 2012;5(3):242-251. doi:10.1016/j.brs.2011.08.005
13. Grimm S, Beck J, Schuepbach D, et al. Imbalance between left and right dorsolateral prefrontal cortex in major depression is linked to negative emotional judgment: an fMRI study in severe major depressive disorder. *Biol Psychiatry*. Feb 15 2008;63(4):369-76. doi:10.1016/j.biopsych.2007.05.033
14. de Berker AO, Bikson M, Bestmann S. Predicting the behavioral impact of transcranial direct current stimulation: issues and limitations. *Front Hum Neurosci*. 2013;7:613. doi:10.3389/fnhum.2013.00613
15. Ko JH, Monchi O, Ptito A, Bloomfield P, Houle S, Strafella AP. Theta burst stimulation-induced inhibition of dorsolateral prefrontal cortex reveals hemispheric asymmetry in striatal dopamine release during a set-shifting task - a TMS-[11C]raclopride PET study. *The European journal of neuroscience*. 2008;28(10):2147-2155. doi:10.1111/j.1460-9568.2008.06501.x

16. Cho SS, Strafella AP. rTMS of the left dorsolateral prefrontal cortex modulates dopamine release in the ipsilateral anterior cingulate cortex and orbitofrontal cortex. *PLoS One*. Aug 21 2009;4(8):e6725. doi:10.1371/journal.pone.0006725
17. West R, Alain C. Age-related decline in inhibitory control contributes to the increased Stroop effect observed in older adults. *Psychophysiology*. Mar 2000;37(2):179-89.
18. Vanderhasselt MA, De Raedt R, Baeken C. Dorsolateral prefrontal cortex and Stroop performance: tackling the lateralization. *Psychon Bull Rev*. Jun 2009;16(3):609-12. doi:10.3758/PBR.16.3.609
19. Peña-Gómez C, Sala-Lonch R, Junqué C, et al. Modulation of large-scale brain networks by transcranial direct current stimulation evidenced by resting-state functional MRI. *Brain Stimul*. Jul 2012;5(3):252-263. doi:10.1016/j.brs.2011.08.006
20. Li Y, Wang L, Jia M, Guo J, Wang H, Wang M. The effects of high-frequency rTMS over the left DLPFC on cognitive control in young healthy participants. *PLoS One*. 2017;12(6):e0179430. doi:10.1371/journal.pone.0179430
21. Sarmiento CI, San-Juan D, Prasath VB. Letter to the Editor: Brief history of transcranial direct current stimulation (tDCS): from electric fishes to microcontrollers. *Psychol Med*. Nov 2016;46(15):3259-3261. doi:10.1017/S0033291716001926
22. Steinberg H. Letter to the Editor: Transcranial direct current stimulation (tDCS) has a history reaching back to the 19th century. *Psychological Medicine*. 2013;43(3):669-671. doi:10.1017/S0033291712002929
23. Hirano M, Kubota S, Koizume Y, Tanaka S, Funase K. Different Effects of Implicit and Explicit Motor Sequence Learning on Latency of Motor Evoked Potential Evoked by Transcranial Magnetic Stimulation on the Primary Motor Cortex. *Front Hum Neurosci*. 2016;10:671. doi:10.3389/fnhum.2016.00671
24. Coppola G, Pierelli F, Schoenen J. Is the cerebral cortex hyperexcitable or hyperresponsive in migraine? *Cephalalgia*. Dec 2007;27(12):1427-39. doi:10.1111/j.1468-2982.2007.01500.x
25. Lloyd DM, Wittkopf PG, Arendsen LJ, Jones AKP. Is Transcranial Direct Current Stimulation (tDCS) Effective for the Treatment of Pain in Fibromyalgia? A Systematic Review and Meta-Analysis. *J Pain*. 2020;21(11-12):1085-1100. doi:10.1016/j.jpain.2020.01.003
26. Zhang R, Lam CLM, Peng X, et al. Efficacy and acceptability of transcranial direct current stimulation for treating depression: A meta-analysis of randomized controlled trials. *Neurosci Biobehav Rev*. Jul 2021;126:481-490. doi:10.1016/j.neubiorev.2021.03.026
27. Oh J, Jang KI, Jeon S, Chae JH. Effect of Self-administered Transcranial Direct Stimulation in Patients with Major Depressive Disorder: A Randomized, Single-blinded Clinical Trial. *Clin Psychopharmacol Neurosci*. Feb 28 2022;20(1):87-96. doi:10.9758/cpn.2022.20.1.87
28. Falcone M, Bernardo L, Ashare RL, et al. Transcranial Direct Current Brain Stimulation Increases Ability to Resist Smoking. *Brain Stimul*. 2016;9(2):191-6. doi:10.1016/j.brs.2015.10.004
29. da Silva MC, Conti CL, Klauss J, et al. Behavioral effects of transcranial direct current stimulation (tDCS) induced dorsolateral prefrontal cortex plasticity in alcohol dependence. *J Physiol Paris*. Dec 2013;107(6):493-502. doi:10.1016/j.jphysparis.2013.07.003
30. Boggio PS, Ferrucci R, Mameli F, et al. Prolonged visual memory enhancement after direct current stimulation in Alzheimer's disease. *Brain Stimul*. Jul 2012;5(3):223-230. doi:10.1016/j.brs.2011.06.006
31. Angius L, Santarnecchi E, Pascual-Leone A, Marcora SM. Transcranial Direct Current Stimulation over the Left Dorsolateral Prefrontal Cortex Improves Inhibitory Control and Endurance Performance in Healthy Individuals. *Neuroscience*. 2019/11/01/ 2019;419:34-45. doi:https://doi.org/10.1016/j.neuroscience.2019.08.052

32. Zhao H, Qiao L, Fan D, et al. Modulation of Brain Activity with Noninvasive Transcranial Direct Current Stimulation (tDCS): Clinical Applications and Safety Concerns. *Front Psychol*. 2017;8:685. doi:10.3389/fpsyg.2017.00685
33. Majdi A, van Boekholdt L, Sadigh-Eteghad S, Mc Laughlin M. A systematic review and meta-analysis of transcranial direct-current stimulation effects on cognitive function in patients with Alzheimer's disease. *Molecular Psychiatry*. 2022/04/01 2022;27(4):2000-2009. doi:10.1038/s41380-022-01444-7
34. Cheng PWC, Louie LLC, Wong YL, et al. The effects of transcranial direct current stimulation (tDCS) on clinical symptoms in schizophrenia: A systematic review and meta-analysis. *Asian J Psychiatr*. Oct 2020;53:102392. doi:10.1016/j.ajp.2020.102392
35. Cardozo D. An intuitive approach to understanding the resting membrane potential. *Adv Physiol Educ*. Dec 2016;40(4):543-547. doi:10.1152/advan.00049.2016
36. Molnar C, & Gair, J. *Concepts of Biology – 1st Canadian Edition* . BCcampus; 2015.
37. Diagram showing the phases of an action potential in relation to the membrane voltage over time. TeachMe Physiology.
38. Neurophysiology module 3. University of Pittsburgh.
39. Stagg CJ, Nitsche MA. Physiological basis of transcranial direct current stimulation. *Neuroscientist*. Feb 2011;17(1):37-53. doi:10.1177/1073858410386614
40. Saturnino GB, Antunes A, Thielscher A. On the importance of electrode parameters for shaping electric field patterns generated by tDCS. *Neuroimage*. Oct 15 2015;120:25-35. doi:10.1016/j.neuroimage.2015.06.067
41. Tanaka T, Isomura Y, Kobayashi K, Hanakawa T, Tanaka S, Honda M. Electrophysiological Effects of Transcranial Direct Current Stimulation on Neural Activity in the Rat Motor Cortex. *Front Neurosci*. 2020;14:495. doi:10.3389/fnins.2020.00495
42. Dmochowski JP, Datta A, Bikson M, Su Y, Parra LC. Optimized multi-electrode stimulation increases focality and intensity at target. *J Neural Eng*. Aug 2011;8(4):046011. doi:10.1088/1741-2560/8/4/046011
43. Sotnikova A, Soff C, Tagliazucchi E, Becker K, Siniatchkin M. Transcranial Direct Current Stimulation Modulates Neuronal Networks in Attention Deficit Hyperactivity Disorder. *Brain Topogr*. Sep 2017;30(5):656-672. doi:10.1007/s10548-017-0552-4
44. Datta A, Truong D, Minhas P, Parra LC, Bikson M. Inter-Individual Variation during Transcranial Direct Current Stimulation and Normalization of Dose Using MRI-Derived Computational Models. *Front Psychiatry*. 2012;3:91. doi:10.3389/fpsyt.2012.00091
45. Zheng X, Alsop DC, Schlaug G. Effects of transcranial direct current stimulation (tDCS) on human regional cerebral blood flow. *Neuroimage*. Sep 01 2011;58(1):26-33. doi:10.1016/j.neuroimage.2011.06.018
46. Ruf SP, Fallgatter AJ, Plewnia C. Augmentation of working memory training by transcranial direct current stimulation (tDCS). *Sci Rep*. Apr 21 2017;7(1):876. doi:10.1038/s41598-017-01055-1
47. Kosko B, Mitaim S. Stochastic resonance in noisy threshold neurons. *Neural Netw*. 2003;16(5-6):755-61. doi:10.1016/S0893-6080(03)00128-X
48. Vignaud P, Mondino M, Poulet E, Palm U, Brunelin J. Duration but not intensity influences transcranial direct current stimulation (tDCS) after-effects on cortical excitability. *Neurophysiol Clin*. Apr 2018;48(2):89-92. doi:10.1016/j.neucli.2018.02.001
49. Nitsche MA, Bikson M. Extending the parameter range for tDCS: Safety and tolerability of 4 mA stimulation. *Brain Stimul*. 2017;10(3):541-542. doi:10.1016/j.brs.2017.03.002
50. van der Groen O, Tang MF, Wenderoth N, Mattingley JB. Stochastic resonance enhances the rate of evidence accumulation during combined brain stimulation and perceptual decision-making. *PLoS Comput Biol*. Jul 2018;14(7):e1006301. doi:10.1371/journal.pcbi.1006301

51. Nitsche MA, Paulus W. Sustained excitability elevations induced by transcranial DC motor cortex stimulation in humans. *Neurology*. Nov 27 2001;57(10):1899-901. doi:10.1212/wnl.57.10.1899
52. Deniz Doruk and Zachary Gray and Gabriela LBaAP-LaFF. Effects of tDCS on executive function in Parkinson's disease. *Neuroscience Letters*. 2014;582:27-31. doi:https://doi.org/10.1016/j.neulet.2014.08.043
53. Jamil A, Nitsche MA. What Effect Does tDCS Have on the Brain? Basic Physiology of tDCS. *Current Behavioral Neuroscience Reports*. 2017/12/01 2017;4(4):331-340. doi:10.1007/s40473-017-0134-5
54. Becker MFP, Tetzlaff C. The biophysical basis underlying the maintenance of early phase long-term potentiation. *PLoS Comput Biol*. Mar 2021;17(3):e1008813. doi:10.1371/journal.pcbi.1008813
55. Islam N, Aftabuddin M, Moriwaki A, Hattori Y, Hori Y. Increase in the calcium level following anodal polarization in the rat brain. *Brain Res*. Jul 03 1995;684(2):206-8. doi:10.1016/0006-8993(95)00434-r
56. Fritsch B, Reis J, Martinowich K, et al. Direct current stimulation promotes BDNF-dependent synaptic plasticity: potential implications for motor learning. *Neuron*. Apr 29 2010;66(2):198-204. doi:10.1016/j.neuron.2010.03.035
57. Lisman J, Yasuda R, Raghavachari S. Mechanisms of CaMKII action in long-term potentiation. *Nat Rev Neurosci*. Feb 15 2012;13(3):169-82. doi:10.1038/nrn3192
58. Díaz-Alonso J, Nicoll RA. AMPA receptor trafficking and LTP: Carboxy-termini, amino-termini and TARPs. *Neuropharmacology*. Oct 01 2021;197:108710. doi:10.1016/j.neuropharm.2021.108710
59. Collingridge GL, Peineau S, Howland JG, Wang YT. Long-term depression in the CNS. *Nat Rev Neurosci*. Jul 2010;11(7):459-73. doi:10.1038/nrn2867
60. Agboada D, Mosayebi-Samani M, Kuo MF, Nitsche MA. Induction of long-term potentiation-like plasticity in the primary motor cortex with repeated anodal transcranial direct current stimulation - Better effects with intensified protocols? *Brain Stimul*. 2020;13(4):987-997. doi:10.1016/j.brs.2020.04.009
61. Hanley JG. The Regulation of AMPA Receptor Endocytosis by Dynamic Protein-Protein Interactions. *Front Cell Neurosci*. 2018;12:362. doi:10.3389/fncel.2018.00362
62. Pikhovych A, Stolberg NP, Jessica Flitsch L, et al. Transcranial Direct Current Stimulation Modulates Neurogenesis and Microglia Activation in the Mouse Brain. *Stem Cells Int*. 2016;2016:2715196. doi:10.1155/2016/2715196
63. Braun R, Klein R, Walter HL, et al. Transcranial direct current stimulation accelerates recovery of function, induces neurogenesis and recruits oligodendrocyte precursors in a rat model of stroke. *Exp Neurol*. May 2016;279:127-136. doi:10.1016/j.expneurol.2016.02.018
64. Ma X, Cheng O, Jiang Q, Yang J, Xiao H, Qiu H. Activation of ephrinb1/EPHB2/MAP-2/NMDAR Mediates Hippocampal Neurogenesis Promoted by Transcranial Direct Current Stimulation in Cerebral-Ischemic Mice. *Neuromolecular Med*. Dec 2021;23(4):521-530. doi:10.1007/s12017-021-08654-2
65. Dubreuil-Vall L, Chau P, Ruffini G, Widge AS, Camprodon JA. tDCS to the left DLPFC modulates cognitive and physiological correlates of executive function in a state-dependent manner. (1876-4754 (Electronic))
66. Accornero N, Capozza M, Pieroni L, Pro S, Davì L, Mecarelli O. EEG mean frequency changes in healthy subjects during prefrontal transcranial direct current stimulation. *J Neurophysiol*. Sep 15 2014;112(6):1367-75. doi:10.1152/jn.00088.2014
67. King BR, Rumpf JJ, Heise KF, et al. Lateralized effects of post-learning transcranial direct current stimulation on motor memory consolidation in older adults: An fMRI investigation. *Neuroimage*. Dec 2020;223:117323. doi:10.1016/j.neuroimage.2020.117323

68. Antal A, Polania R, Schmidt-Samoa C, Dechent P, Paulus W. Transcranial direct current stimulation over the primary motor cortex during fMRI. *Neuroimage*. Mar 15 2011;55(2):590-6. doi:10.1016/j.neuroimage.2010.11.085
69. Xu K, Liu, Y., Zhan, Y., Ren, J., Jiang, T. BRANT: A Versatile and Extendable Resting-State fMRI Toolkit . Front Neuroinform, 12:52; 2018.
70. Barbey AK, Koenigs M, Grafman J. Dorsolateral prefrontal contributions to human working memory. *Cortex*. May 2013;49(5):1195-205. doi:10.1016/j.cortex.2012.05.022
71. Owen AM, Downes JJ, Sahakian BJ, Polkey CE, Robbins TW. Planning and spatial working memory following frontal lobe lesions in man. *Neuropsychologia*. 1990;28(10):1021-34. doi:10.1016/0028-3932(90)90137-d
72. van Asselen M, Kessels RP, Neggers SF, Kappelle LJ, Frijns CJ, Postma A. Brain areas involved in spatial working memory. *Neuropsychologia*. 2006;44(7):1185-94. doi:10.1016/j.neuropsychologia.2005.10.005
73. Curtis CE, D'Esposito M. Persistent activity in the prefrontal cortex during working memory. *Trends Cogn Sci*. Sep 2003;7(9):415-423. doi:10.1016/s1364-6613(03)00197-9
74. D'Esposito M, Cooney JW, Gazzaley A, Gibbs SE, Postle BR. Is the prefrontal cortex necessary for delay task performance? Evidence from lesion and FMRI data. *J Int Neuropsychol Soc*. Mar 2006;12(2):248-60. doi:10.1017/S1355617706060322
75. Petrides M. Dissociable roles of mid-dorsolateral prefrontal and anterior inferotemporal cortex in visual working memory. *J Neurosci*. Oct 01 2000;20(19):7496-503. doi:10.1523/JNEUROSCI.20-19-07496.2000
76. Shallice T, Burgess PW. Deficits in strategy application following frontal lobe damage in man. *Brain*. Apr 1991;114 (Pt 2):727-41. doi:10.1093/brain/114.2.727
77. Lombardi WJ, Andreason PJ, Sirocco KY, et al. Wisconsin Card Sorting Test Performance Following Head Injury: Dorsolateral Fronto-Striatal Circuit Activity Predicts Perseveration. *Journal of Clinical and Experimental Neuropsychology*. 1999/02/01 1999;21(1):2-16. doi:10.1076/jcen.21.1.2.940
78. Greene JD, Nystrom LE, Engell AD, Darley JM, Cohen JD. The neural bases of cognitive conflict and control in moral judgment. *Neuron*. Oct 14 2004;44(2):389-400. doi:10.1016/j.neuron.2004.09.027
79. Zheng H, Lu X, Huang D. tDCS Over DLPFC Leads to Less Utilitarian Response in Moral-Personal Judgment. *Front Neurosci*. 2018;12:193. doi:10.3389/fnins.2018.00193
80. Heekeren HR, Wartenburger I, Schmidt H, Schwintowski HP, Villringer A. An fMRI study of simple ethical decision-making. *Neuroreport*. Jul 01 2003;14(9):1215-9. doi:10.1097/00001756-200307010-00005
81. Oldrati V, Patricelli J, Colombo B, Antonietti A. The role of dorsolateral prefrontal cortex in inhibition mechanism: A study on cognitive reflection test and similar tasks through neuromodulation. *Neuropsychologia*. Oct 2016;91:499-508. doi:10.1016/j.neuropsychologia.2016.09.010
82. Kadota H, Sekiguchi H, Takeuchi S, Miyazaki M, Kohno Y, Nakajima Y. The role of the dorsolateral prefrontal cortex in the inhibition of stereotyped responses. *Exp Brain Res*. Jun 2010;203(3):593-600. doi:10.1007/s00221-010-2269-4
83. Floden D, Stuss DT. Inhibitory control is slowed in patients with right superior medial frontal damage. *J Cogn Neurosci*. Nov 2006;18(11):1843-9. doi:10.1162/jocn.2006.18.11.1843
84. MacDonald AW, Cohen JD, Stenger VA, Carter CS. Dissociating the role of the dorsolateral prefrontal and anterior cingulate cortex in cognitive control. *Science*. Jun 09 2000;288(5472):1835-8. doi:10.1126/science.288.5472.1835
85. Marek S, Dosenbach NUF. The frontoparietal network: function, electrophysiology, and importance of individual precision mapping. *Dialogues Clin Neurosci*. Jun 2018;20(2):133-140. doi:10.31887/DCNS.2018.20.2/smarek

86. Seeley WW, Menon V, Schatzberg AF, et al. Dissociable intrinsic connectivity networks for salience processing and executive control. *J Neurosci*. Feb 28 2007;27(9):2349-56. doi:10.1523/JNEUROSCI.5587-06.2007
87. McLaughlin NCR, Malloy P. Dorsolateral Prefrontal Cortex. In: Kreutzer J, DeLuca J, Caplan B, eds. *Encyclopedia of Clinical Neuropsychology*. Springer International Publishing; 2017:1-5.
88. Zaehle T, Sandmann P, Thorne JD, Jäncke L, Herrmann CS. Transcranial direct current stimulation of the prefrontal cortex modulates working memory performance: combined behavioural and electrophysiological evidence. *BMC Neurosci*. Jan 06 2011;12:2. doi:10.1186/1471-2202-12-2
89. Mulquiney PG, Hoy KE, Daskalakis ZJ, Fitzgerald PB. Improving working memory: exploring the effect of transcranial random noise stimulation and transcranial direct current stimulation on the dorsolateral prefrontal cortex. *Clin Neurophysiol*. Dec 2011;122(12):2384-9. doi:10.1016/j.clinph.2011.05.009
90. Jeon SY, Han SJ. Improvement of the working memory and naming by transcranial direct current stimulation. *Ann Rehabil Med*. Oct 2012;36(5):585-95. doi:10.5535/arm.2012.36.5.585
91. Mylius V, Jung M, Menzler K, et al. Effects of transcranial direct current stimulation on pain perception and working memory. *Eur J Pain*. Aug 2012;16(7):974-82. doi:10.1002/j.1532-2149.2011.00105.x
92. Meiron O, Lavidor M. Unilateral prefrontal direct current stimulation effects are modulated by working memory load and gender. *Brain Stimul*. May 2013;6(3):440-7. doi:10.1016/j.brs.2012.05.014
93. Hassanzahraee M, Nitsche MA, Zoghi M, Jaberzadeh S. Determination of anodal tDCS duration threshold for reversal of corticospinal excitability: An investigation for induction of counter-regulatory mechanisms. *Brain Stimul*. 2020;13(3):832-839. doi:10.1016/j.brs.2020.02.027
94. Dockery CA, Hueckel-Weng R, Birbaumer N, Plewnia C. Enhancement of planning ability by transcranial direct current stimulation. *J Neurosci*. Jun 03 2009;29(22):7271-7. doi:10.1523/JNEUROSCI.0065-09.2009
95. Vannorsdall TD, Schretlen DJ, Andrejczuk M, et al. Altering automatic verbal processes with transcranial direct current stimulation. *Front Psychiatry*. 2012;3:73. doi:10.3389/fpsyt.2012.00073
96. Leite J, Carvalho S, Fregni F, Boggio PS, Gonçalves OF. The effects of cross-hemispheric dorsolateral prefrontal cortex transcranial direct current stimulation (tDCS) on task switching. *Brain Stimul*. Jul 2013;6(4):660-7. doi:10.1016/j.brs.2012.10.006
97. Feeser M, Prehn K, Kazzer P, Mungee A, Bajbouj M. Transcranial Direct Current Stimulation Enhances Cognitive Control During Emotion Regulation. *Brain Stimulation*. 2014/01/01/ 2014;7(1):105-112. doi:https://doi.org/10.1016/j.brs.2013.08.006
98. Sela T, Ivry RB, Lavidor M. Prefrontal control during a semantic decision task that involves idiom comprehension: a transcranial direct current stimulation study. *Neuropsychologia*. Jul 2012;50(9):2271-80. doi:10.1016/j.neuropsychologia.2012.05.031
99. Keeser D, Meindl T, Bor J, et al. Prefrontal transcranial direct current stimulation changes connectivity of resting-state networks during fMRI. *J Neurosci*. Oct 26 2011;31(43):15284-93. doi:10.1523/JNEUROSCI.0542-11.2011
100. Weber MJ, Messing SB, Rao H, Detre JA, Thompson-Schill SL. Prefrontal transcranial direct current stimulation alters activation and connectivity in cortical and subcortical reward systems: a tDCS-fMRI study. *Hum Brain Mapp*. Aug 2014;35(8):3673-86. doi:10.1002/hbm.22429
101. Sacca V, Maleki N, Wen Y, Hodges S, Kong J. Modulation Effects of Repeated Transcranial Direct Current Stimulation at the Dorsolateral Prefrontal Cortex: A Pulsed Continuous Arterial Spin Labeling Study. *Brain Sci*. Feb 25 2023;13(3)doi:10.3390/brainsci13030395
102. Bunai T, Hirosawa T, Kikuchi M, et al. tDCS-induced modulation of GABA concentration and dopamine release in the human brain: A combination study of magnetic resonance spectroscopy and positron emission tomography. *Brain Stimul*. 2021;14(1):154-160. doi:10.1016/j.brs.2020.12.010

103. Friston KJ. Functional and effective connectivity in neuroimaging: A synthesis. *Human Brain Mapping*. 1994;2(1-2):56-78. doi:https://doi.org/10.1002/hbm.460020107
104. Soares JM, Magalhães R, Moreira PS, et al. A Hitchhiker's Guide to Functional Magnetic Resonance Imaging. *Front Neurosci*. 2016;10:515. doi:10.3389/fnins.2016.00515
105. Kim S-G, Bandettini PA. Principles of BOLD Functional MRI. In: Faro SH, Mohamed FB, Law M, Ulmer JT, eds. *Functional Neuroradiology: Principles and Clinical Applications*. Springer US; 2012:293-303.
106. Venkat P, Chopp M, Chen J. New insights into coupling and uncoupling of cerebral blood flow and metabolism in the brain. *Croat Med J*. Jun 30 2016;57(3):223-8. doi:10.3325/cmj.2016.57.223
107. Hillman EM. Coupling mechanism and significance of the BOLD signal: a status report. *Annu Rev Neurosci*. 2014;37:161-81. doi:10.1146/annurev-neuro-071013-014111
108. Grover VP, Tognarelli JM, Crossey MM, Cox IJ, Taylor-Robinson SD, McPhail MJ. Magnetic Resonance Imaging: Principles and Techniques: Lessons for Clinicians. *J Clin Exp Hepatol*. Sep 2015;5(3):246-55. doi:10.1016/j.jceh.2015.08.001
109. Barth M, Moser E. Proton NMR relaxation times of human blood samples at 1.5 T and implications for functional MRI. *Cell Mol Biol (Noisy-le-grand)*. Jul 1997;43(5):783-91.
110. Biswal B, Yetkin FZ, Haughton VM, Hyde JS. Functional connectivity in the motor cortex of resting human brain using echo-planar MRI. *Magn Reson Med*. Oct 1995;34(4):537-41. doi:10.1002/mrm.1910340409
111. Zhan X, Yu R. A Window into the Brain: Advances in Psychiatric fMRI. *Biomed Res Int*. 2015;2015:542467. doi:10.1155/2015/542467
112. Lee MH, Smyser CD, Shimony JS. Resting-state fMRI: a review of methods and clinical applications. *AJNR Am J Neuroradiol*. Oct 2013;34(10):1866-72. doi:10.3174/ajnr.A3263
113. Cole DM, Smith SM, Beckmann CF. Advances and pitfalls in the analysis and interpretation of resting-state FMRI data. *Front Syst Neurosci*. 2010;4:8. doi:10.3389/fnsys.2010.00008
114. Borogovac A, Asllani I. Arterial Spin Labeling (ASL) fMRI: advantages, theoretical constrains, and experimental challenges in neurosciences. *Int J Biomed Imaging*. 2012;2012:818456. doi:10.1155/2012/818456
115. Alhindi A. *The Functional Connectivity of the Caudate Nucleus is*

Correlated with Cognitive Performance in

Parkinson's Disease Patients. University of Manitoba; 2018.
116. Soleimani G, Towhidkhah F, Oghabian MA, Ekhtiari H. DLPFC stimulation alters large-scale brain networks connectivity during a drug cue reactivity task: A tDCS-fMRI study. *Front Syst Neurosci*. 2022;16:956315. doi:10.3389/fnsys.2022.956315
117. Leaver AM, Gonzalez S, Vasavada M, et al. Modulation of brain networks during MR-compatible transcranial direct current stimulation. *Neuroimage*. Apr 15 2022;250:118874. doi:10.1016/j.neuroimage.2022.118874
118. Stagg CJ, Lin RL, Mezue M, et al. Widespread modulation of cerebral perfusion induced during and after transcranial direct current stimulation applied to the left dorsolateral prefrontal cortex. *J Neurosci*. Jul 10 2013;33(28):11425-31. doi:10.1523/JNEUROSCI.3887-12.2013
119. Le Reste PJ, Haegelen C, Gibaud B, Moreau T, Morandi X. Connections of the dorsolateral prefrontal cortex with the thalamus: a probabilistic tractography study. *Surg Radiol Anat*. Aug 2016;38(6):705-10. doi:10.1007/s00276-015-1603-8
120. Liang P, Wang Z, Yang Y, Jia X, Li K. Functional disconnection and compensation in mild cognitive impairment: evidence from DLPFC connectivity using resting-state fMRI. *PLoS One*. 2011;6(7):e22153. doi:10.1371/journal.pone.0022153

121. Huster RJ, Wolters C, Wollbrink A, et al. Effects of anterior cingulate fissurization on cognitive control during stroop interference. *Hum Brain Mapp*. Apr 2009;30(4):1279-89. doi:10.1002/hbm.20594
122. Cutuli D. Cognitive reappraisal and expressive suppression strategies role in the emotion regulation: an overview on their modulatory effects and neural correlates. *Front Syst Neurosci*. 2014;8:175. doi:10.3389/fnsys.2014.00175
123. Vogt BA. Midcingulate cortex: Structure, connections, homologies, functions and diseases. *J Chem Neuroanat*. Jul 2016;74:28-46. doi:10.1016/j.jchemneu.2016.01.010
124. Jog MS, Kim E, Anderson C, et al. In-vivo imaging of targeting and modulation of depression-relevant circuitry by transcranial direct current stimulation: a randomized clinical trial. *Transl Psychiatry*. Feb 24 2021;11(1):138. doi:10.1038/s41398-021-01264-3
125. Saleh B. Medical Imaging Modalities: Positron Emission Tomography (PET).
126. Fukai M, Bunai T, Hirosawa T, et al. Endogenous dopamine release under transcranial direct-current stimulation governs enhanced attention: a study with positron emission tomography. *Transl Psychiatry*. Mar 15 2019;9(1):115. doi:10.1038/s41398-019-0443-4
127. Fonteneau C, Redoute J, Haesebaert F, et al. Frontal Transcranial Direct Current Stimulation Induces Dopamine Release in the Ventral Striatum in Human. *Cereb Cortex*. Jul 01 2018;28(7):2636-2646. doi:10.1093/cercor/bhy093
128. Gordon PC, Zrenner C, Desideri D, et al. Modulation of cortical responses by transcranial direct current stimulation of dorsolateral prefrontal cortex: A resting-state EEG and TMS-EEG study. *Brain Stimul*. 2018;11(5):1024-1032. doi:10.1016/j.brs.2018.06.004
129. Boudewyn M, Roberts BM, Mizrak E, Ranganath C, Carter CS. Prefrontal transcranial direct current stimulation (tDCS) enhances behavioral and EEG markers of proactive control. *Cogn Neurosci*. 2019;10(2):57-65. doi:10.1080/17588928.2018.1551869
130. Hermann B, Raimondo F, Hirsch L, et al. Combined behavioral and electrophysiological evidence for a direct cortical effect of prefrontal tDCS on disorders of consciousness. *Sci Rep*. Mar 09 2020;10(1):4323. doi:10.1038/s41598-020-61180-2
131. Keeser D, Padberg F, Reisinger E, et al. Prefrontal direct current stimulation modulates resting EEG and event-related potentials in healthy subjects: a standardized low resolution tomography (sLORETA) study. *Neuroimage*. Mar 15 2011;55(2):644-57. doi:10.1016/j.neuroimage.2010.12.004
132. Nasreddine ZS, Phillips NA, Bédirian V, et al. The Montreal Cognitive Assessment, MoCA: a brief screening tool for mild cognitive impairment. *J Am Geriatr Soc*. Apr 2005;53(4):695-9. doi:10.1111/j.1532-5415.2005.53221.x
133. Golden CJ. A Manual for the Clinical and Experimental Use of the Stroop Color and Word Test. . Chicago: Stoelting Co; 1978.
134. Beck AT, Steer, R.A., & Brown, G.K. Manual for the Beck

Depression Inventory-II. San Antonio Texas: Psychological Corporation; 1996.
135. CSRC. ANAM GNS Battery: Administration Manual. Cognitive Science Research Center, University of Oklahoma, Norman, OK.2013.
136. Whitfield-Gabrieli S, Nieto-Castanon A. Conn: a functional connectivity toolbox for correlated and anticorrelated brain networks. *Brain Connect*. 2012;2(3):125-41. doi:10.1089/brain.2012.0073
137. Scrivener CL, Reader AT. Variability of EEG electrode positions and their underlying brain regions: visualizing gel artifacts from a simultaneous EEG-fMRI dataset. *Brain and Behavior*. 2022;12(2):e2476. doi:https://doi.org/10.1002/brb3.2476
138. Wang Z, Aguirre GK, Rao H, et al. Empirical optimization of ASL data analysis using an ASL data processing toolbox: ASLtbx. *Magn Reson Imaging*. Feb 2008;26(2):261-9. doi:10.1016/j.mri.2007.07.003

139. Greeley B, Seidler RD. Differential effects of left and right prefrontal cortex anodal transcranial direct current stimulation during probabilistic sequence learning. *J Neurophysiol*. May 01 2019;121(5):1906-1916. doi:10.1152/jn.00795.2018
140. Nalls MA, Blauwendraat C, Vallerga CL, et al. Identification of novel risk loci, causal insights, and heritable risk for Parkinson's disease: a meta-analysis of genome-wide association studies. *Lancet Neurol*. 12 2019;18(12):1091-1102. doi:10.1016/S1474-4422(19)30320-5
141. Liu W, Mao Y, Wei D, et al. Structural Asymmetry of Dorsolateral Prefrontal Cortex Correlates with Depressive Symptoms: Evidence from Healthy Individuals and Patients with Major Depressive Disorder. *Neurosci Bull*. Jun 2016;32(3):217-26. doi:10.1007/s12264-016-0025-x
142. Sadleir RJ, Vannorsdall TD, Schretlen DJ, Gordon B. Transcranial direct current stimulation (tDCS) in a realistic head model. *NeuroImage*. 2010/07/15/ 2010;51(4):1310-1318. doi:https://doi.org/10.1016/j.neuroimage.2010.03.052
143. Sotero RC, Trujillo-Barreto NJ. Modelling the role of excitatory and inhibitory neuronal activity in the generation of the BOLD signal. *Neuroimage*. Mar 2007;35(1):149-65. doi:10.1016/j.neuroimage.2006.10.027
144. Glick SD, Ross DA, Hough LB. Lateral asymmetry of neurotransmitters in human brain. *Brain Res*. Feb 18 1982;234(1):53-63. doi:10.1016/0006-8993(82)90472-3
145. Seibt O, Brunoni AR, Huang Y, Bikson M. The Pursuit of DLPFC: Non-neuronavigated Methods to Target the Left Dorsolateral Pre-frontal Cortex With Symmetric Bicephalic Transcranial Direct Current Stimulation (tDCS). *Brain Stimul*. 2015 May-Jun 2015;8(3):590-602. doi:10.1016/j.brs.2015.01.401
146. Peterchev AV, Wagner TA, Miranda PC, et al. Fundamentals of transcranial electric and magnetic stimulation dose: definition, selection, and reporting practices. *Brain Stimul*. Oct 2012;5(4):435-53. doi:10.1016/j.brs.2011.10.001
147. Gomez-Tames J, Asai A, Hirata A. Significant group-level hotspots found in deep brain regions during transcranial direct current stimulation (tDCS): A computational analysis of electric fields. *Clin Neurophysiol*. 03 2020;131(3):755-765. doi:10.1016/j.clinph.2019.11.018
148. Utevsky AV, Smith DV, Huettel SA. Precuneus is a functional core of the default-mode network. *J Neurosci*. Jan 15 2014;34(3):932-40. doi:10.1523/JNEUROSCI.4227-13.2014
149. Whitfield-Gabrieli S, Ford JM. Default mode network activity and connectivity in psychopathology. *Annu Rev Clin Psychol*. 2012;8:49-76. doi:10.1146/annurev-clinpsy-032511-143049
150. Menon V. Large-scale brain networks and psychopathology: a unifying triple network model. *Trends Cogn Sci*. Oct 2011;15(10):483-506. doi:10.1016/j.tics.2011.08.003
151. Stoodley CJ. The cerebellum and cognition: evidence from functional imaging studies. *Cerebellum*. Jun 2012;11(2):352-65. doi:10.1007/s12311-011-0260-7
152. Li LM, Violante IR, Leech R, et al. Brain state and polarity dependent modulation of brain networks by transcranial direct current stimulation. *Hum Brain Mapp*. Feb 15 2019;40(3):904-915. doi:10.1002/hbm.24420
153. Amadi U, Ilie A, Johansen-Berg H, Stagg CJ. Polarity-specific effects of motor transcranial direct current stimulation on fMRI resting state networks. *Neuroimage*. Mar 2014;88(100):155-61. doi:10.1016/j.neuroimage.2013.11.037
154. Perrotta D, Bianco V, Berchicci M, Quinzi F, Perri RL. Anodal tDCS over the dorsolateral prefrontal cortex reduces Stroop errors. A comparison of different tasks and designs. *Behav Brain Res*. 05 07 2021;405:113215. doi:10.1016/j.bbr.2021.113215
155. Friehs MA, Frings C. Pimping inhibition: Anodal tDCS enhances stop-signal reaction time. *J Exp Psychol Hum Percept Perform*. Dec 2018;44(12):1933-1945. doi:10.1037/xhp0000579
156. Sakai H, Uchiyama Y, Shin D, Hayashi MJ, Sadato N. Neural activity changes associated with impulsive responding in the sustained attention to response task. *PLoS One*. 2013;8(6):e67391. doi:10.1371/journal.pone.0067391

157. Ko JH, Monchi O, Ptito A, Petrides M, Strafella AP. Repetitive Transcranial Magnetic Stimulation of Dorsolateral Prefrontal Cortex Affects Performance of the Wisconsin Card Sorting Task during Provision of Feedback. *Int J Biomed Imaging*. 2008;2008:143238.
158. Mansouri FA, Buckley MJ, Mahboubi M, Tanaka K. Behavioral consequences of selective damage to frontal pole and posterior cingulate cortices. *Proc Natl Acad Sci U S A*. Jul 21 2015;112(29):E3940-9. doi:10.1073/pnas.1422629112
159. Baumert A, Buchholz N, Zinkernagel A, et al. Causal underpinnings of working memory and Stroop interference control: Testing the effects of anodal and cathodal tDCS over the left DLPFC. doi:10.3758/s13415-019-00726-y
160. Frings C, Brinkmann T, Friehs MA, van Lipzig T. Single session tDCS over the left DLPFC disrupts interference processing. *Brain Cogn*. 02 2018;120:1-7. doi:10.1016/j.bandc.2017.11.005
161. Ole S, Dennis T, Niranjan K, Yu H, Marom B. Computational Finite Element Method (FEM) forward modeling workflow for transcranial Direct Current Stimulation (tDCS) current flow on MRI-derived head: Simpleware and COMSOL Multiphysics tutorial. *bioRxiv*. 2019:704940. doi:10.1101/704940